Biotechnology Advances 69 (2023) 108264

Contents lists available at ScienceDirect

Biotechnology Advances

journal homepage: www.elsevier.com/locate/biotechadv

Research review paper

Cupriavidus necator as a platform for polyhydroxyalkanoate production: An overview of strains, metabolism, and modeling approaches

Maria Silvia Morlino [a], Rebecca Serna García [b], Filippo Savio [a], Guido Zampieri [a], Tomas Morosinotto [a], Laura Treu [a,*], Stefano Campanaro [a]

[a] Department of Biology, University of Padua, via U. Bassi 58/b, 35131 Padova, Italy
[b] CALAGUA - Unidad Mixta UV-UPV, Departament d'Enginyeria Química, Universitat de València, Avinguda de la Universitat s/n, 46100 Burjassot, Valencia, Spain

ARTICLE INFO

Keywords:
Cupriavidus necator
Strain diversity
Polyhydroxyalkanoates
Waste valorization
CO_2 fixation
Metabolic modeling
Flux balance analysis

ABSTRACT

Cupriavidus necator is a bacterium with a high phenotypic diversity and versatile metabolic capabilities. It has been extensively studied as a model hydrogen oxidizer, as well as a producer of polyhydroxyalkanoates (PHA), plastic-like biopolymers with a high potential to substitute petroleum-based materials. Thanks to its adaptability to diverse metabolic lifestyles and to the ability to accumulate large amounts of PHA, *C. necator* is employed in many biotechnological processes, with particular focus on PHA production from waste carbon sources. The large availability of genomic information has enabled a characterization of *C. necator*'s metabolism, leading to the establishment of metabolic models which are used to devise and optimize culture conditions and genetic engineering approaches.

In this work, the characteristics of available *C. necator* strains and genomes are reviewed, underlining how a thorough comprehension of the genetic variability of *C. necator* is lacking and it could be instrumental for wider application of this microorganism. The metabolic paradigms of *C. necator* and how they are connected to PHA production and accumulation are described, also recapitulating the variety of carbon substrates used for PHA accumulation, highlighting the most promising strategies to increase the yield. Finally, the review describes and critically analyzes currently available genome-scale metabolic models and reduced metabolic network applications commonly employed in the optimization of PHA production. Overall, it appears that the capacity of *C. necator* of performing CO_2 bioconversion to PHA is still underexplored, both in biotechnological applications and in metabolic modeling. However, the accurate characterization of this organism and the efforts in using it for gas fermentation can help tackle this challenging perspective in the future.

1. Introduction

Cupriavidus necator (previously known as *Wautersia eutropha*, *Ralstonia eutropha* and *Alcaligenes eutrophus*) is a Gram-negative bacterium belonging to the *Burkholderiaceae* family. According to the information in the literature and in public strains collections such as Leibniz Institute DSMZ collection (https://www.dsmz.de/) and ATCC (https://www.atcc.org/), it was isolated independently from several environments, including sludge from ponds and rivers, forest and paddy field soil, rhizosphere of plants, root nodules, and human clinical specimens (Moriuchi et al., 2019). The variety of environments where *C. necator* was isolated reflects its versatile metabolic capabilities: this species is able to grow as a chemolithotroph and heterotroph, in both aerobic and anaerobic environments. Heterotrophic growth occurs using a wide array of carbon sources, and even in the case of chemolithotrophic growth, CO_2 and formate can be used (Sohn et al., 2021). Of special

Abbreviations: 3HB, 3-hydroxybutyrate; 3HHx, 3-hydroxyhexanoate; 3HV, 3-hydroxyvalerate; CBB, Calvin-Benson-Bassham; CDW, cell dry weight; CGP, crude glycerol phase; ED, Entner-Doudoroff; EM, elementary mode; EMP, Embden-Meyerhof-Parnas; (D)FBA, (dynamic) flux balance analysis; G-6-PDH, glucose-6-phosphate-dehydrogenase; GSMM, genome-scale metabolic model; HCM, hybrid cybernetic model; HMM, hidden Markov model; KEGG, Kyoto Encyclopedia of Genes and Genomes; P(3HB), poly(3-hydroxybutyrate); P(4HB), poly(4-hydroxybutyrate); PHA, polyhydroxyalkanoates; PHB, polyhydroxybutyrate; PHBV, poly(3-hydroxybutyrate-co-3-hydroxyvalerate); PPP, pentose phosphate pathway; rRNA, ribosomal RNA; SFAE, saturated share of biodiesel; TCA, tricarboxylic acid cycle; VFA, volatile fatty acids.

* Corresponding author.
E-mail address: laura.treu@unipd.it (L. Treu).

https://doi.org/10.1016/j.biotechadv.2023.108264
Received 14 July 2023; Received in revised form 18 September 2023; Accepted 26 September 2023
Available online 27 September 2023

biotechnological interest is that *C. necator* accumulates intracellular granules of poly(3-hydroxybutyrate) (P[3HB], or PHB) and other polyhydroxyalkanoates (PHA) as a carbon reservoir when other nutrient elements are lacking (Schlegel et al., 1961). PHA are highly interesting to be employed as substitutes to petroleum-based plastics, making *C. necator* an excellent target species for the industrial production of these polymers. In the light of the impending global crisis related to plastic pollution, growing CO_2 emissions, and the subsequent effects on climate change, a conspicuous amount of research is being addressed at devising processes that employ waste streams as feedstocks for bioconversion to products of industrial interest. In this regard, *C. necator* holds great potential as its growth on organic waste streams has been demonstrated (Section 4.1), allowing their valorization; plus, chemolithotrophic growth on CO_2-rich gaseous streams from industrial activities could prevent emissions or reduce the impact on the atmosphere, while also providing biodegradable plastics.

The flexibility of *C. necator* as a platform for value-added chemical production and its capability to fix CO_2 has encouraged efforts to establish comprehensive and well-curated genome-scale metabolic models (GSMMs) to simulate growth with different carbon sources and conditions, as well as *in silico* gene knockouts. GSMMs are mathematical representations of all known biochemical reactions in an organism. Each reaction is characterized by a rate and a stoichiometry which allow calculating how fast compounds are consumed and produced given a set of biological or physico-chemical constraints (Orth et al., 2010). These models hold great potential for simulating the effects of environmental conditions, feedstock, and even genetic engineering on the overall metabolism. Because of their ability to predict the impact of many parameters *in silico*, GSMMs and akin models have been widely employed to explore strategies to improve PHA and PHB yields and represent a major tool for productivity optimization. However, due to their scale, reliable models require extensive manual curation and validation with multi-omic data.

Due to independent isolations of the organism in diverse environments, as well as the paradigm shift in taxonomic classification, transitioning from morphological and physiological principles to marker genes, and whole genome comparisons, *C. necator* can be found in the literature and databases under different names. Hence, it is useful to recapitulate the story of its taxonomic reassignments in over 80 years in order to organize available information about this important species more efficiently, enhancing data retrieval and model development (Moriuchi et al., 2019). Further, given the wide variety of natural and engineered strains and the complexity of metabolism, a systematic and detailed account of relevant knowledge is of primary importance for a better use of this microorganism for the exploitation of waste streams.

This review provides an overview of *C. necator* focusing on its metabolism and applications, which can aid in planning data-driven experiments and implementing metabolic models. First, the review summarizes current knowledge on *C. necator* strains and deposited genomes, discussing the accuracy of taxonomic assignments. Then, the metabolic paradigms of wild-type *C. necator* are described in detail, and metabolic regulation of PHA production is elucidated. Subsequently, efforts to maximize PHA yield in a variety of circular economy applications are discussed, including investigations on the operational parameters and metabolic engineering attempts. Finally, a recapitulation of available metabolic models is presented, highlighting their importance in the product optimization.

2. Taxonomy and phylogenetic diversity

The genome of *C. necator*, like that of many *Burkholderiaceae*, is multipartite. Most strains have three replicons: chromosome 1, chromosome 2, and megaplasmid pHG1. Chromosome 1 encodes most housekeeping genes, while the other two replicons include most of the genes necessary for chemolithotrophic and anaerobic lifestyles, as well as alternative substrate uptake (Jahn et al., 2021; Fricke et al., 2009; Pohlmann et al., 2006).

The taxonomic classification of *C. necator* underwent several changes since its first isolation in 1957. The first published studies classified it as *Hydrogenomonas eutropha*, due to the capability of the bacterium to grow chemolithotrophically on a mixture of hydrogen, oxygen, and CO_2. Indeed, the genus *Hydrogenomonas*, established in 1909, encompassed all species capable of hydrogen oxidation (Davis et al., 1969; Repaske, 1962; Schlegel et al., 1961). However, due to the heterogeneity of the species assigned to this genus, its disgregation was proposed in 1969, and the name was changed to *Alcaligenes eutrophus* (Davis et al., 1969). The species name was changed again upon a rearrangement of the *Burkholderia* family, becoming *Ralstonia eutropha*, where *Ralstonia* was a novel genus encompassing the former *A. eutrophus* and two *Burkholderia* species (Yabuuchi et al., 1995). The *Ralstonia* genus was later split in two different genera, changing *Ralstonia eutropha* to *Wautersia eutropha* (Vaneechoutte et al., 2004). During the same year, a DNA-DNA hybridization experiment confirmed that *W. eutropha* was in fact the same species as another isolate obtained by Makkar and Casida in 1987, named *Cupriavidus necator*. The decision to assign this isolate to a new genus and species was made based on the predatory activity that it displayed, which was not found in the *Alcaligenes* genus (Makkar and Casida, 1987). However, this trait was later proven to be linked to the presence of a specific plasmid. Therefore, in compliance with the rules established in the International Code of Nomenclature of Prokaryotes (International Code of Nomenclature of Prokaryotes, 2019), *W. eutropha* in 2004 was finally renamed *C. necator*, since this was the first published valid taxonomic name for the species. Thus, the isolate by Makkar and Casida, dubbed N-1, became the nomenclatural type for the species (Vandamme and Coenye, 2004; Makkar and Casida, 1987).

Many *C. necator* strains have been isolated over time. As of May 2023, 33 strains are listed in the DSMZ, of which 14 are wild-type isolates, while the remaining 19 strains are derivatives of the isolates by means of mutagenesis or genetic engineering. It has been ascertained for some of the isolates that they differ slightly in terms of physiological properties and PHA synthesis characteristics (Bowien and Schlegel, 1981; Schlegel et al., 1961). Several other isolates, not listed in the DSMZ, are present in the NCBI database; indeed, out of the 14 *C. necator* genomes available in the RefSeq database, 11 belong to strains that are not listed in the collection (Table 1). There are however very few studies where physiological or genomic data from different strains are compared. A considerable amount of literature about isolates dates to the 1970's or earlier, and the original manuscripts describing physiological characteristics are only available in German. Out of the 14 strains with a publicly available genome sequence, 7 were not associated with any publication, and no additional information about them was available in the literature. Three entries are from soil isolates with the ability to degrade aromatic and chlorinated compounds. The remaining entries are sequences of strains available in the DSMZ. In addition to the strains directly listed as *C. necator*, one strain named KK10 was considered in the analysis described below, since it is listed as *Cupriavidus* sp. in RefSeq, but it is described as *C. necator* in the corresponding paper (Mori et al., 2021).

To get an overview of the sequenced genomes present in RefSeq, their phylogeny was inferred via multi-locus sequence analysis and average nucleotide identity (ANI) in order to clarify the relationships among the different strains. The 16S ribosomal RNA (rRNA) sequences were also extrapolated and aligned (Fig. 1). Pairwise ANI was calculated between all genomes with the FastANI library (Jain et al., 2018, available at https://github.com/ParBLiSS/FastANI) and a dendrogram was constructed in Python with the SciPy library (Virtanen et al., 2020) using the Unweighted Pair Group Method with Arithmetic Mean clustering method (Bar-Joseph et al., 2001), with the distance values defined as 100 - ANI. 16S regions were extracted via Hidden Markov Model (HMM) search. The HMM used is the file "bac.ssu.rnammer.hmm" from RNAmmer (https://services.healthtech.dtu.dk/services/RNAmmer-1.2/), which was built from a set of known bacterial 16S rRNA regions. The

Table 1
Currently known *C. necator* strains in the Leibniz Institute DSMZ collection and the NCBI RefSeq database. Known isolates have their strain name in bold. When multiple assemblies are present for the same strain, the year of submission is reported. ATCC catalog numbers are reported when available.

DSMZ catalog no.	ATCC catalog no.	Strain name	Assembly ID	Notes	References
DSM 428	ATCC 17699	**H16**	RefSeq ID: GCF_000009285.2 (2006) RefSeq ID: GCF_004798725.1 (2019) RefSeq ID: GCF_016127575.1 (2020)	Isolated from sludge. The 2020 assembly is noted in RefSeq under strain name "FDAARGOS_1030".	Little et al., 2019 Sichtig et al., 2019 Pohlmann et al., 2006 Schlegel et al., 1961
DSM 529	ATCC 23442	**H1**	–	Isolated from sludge from a garden pond	Bartha, 1962 Schlegel et al., 1961
DSM 530	ATCC 17700	**H20**	–	Isolated from soil	Schlegel et al., 1961
DSM 531	ATCC 17697	**335, R-10-e**	RefSeq ID: GCF_001598755.1	Isolated from soil. Formerly type strain of *Wautersia eutropha*. Noted in RefSeq under strain name "NBRC 102504″	Johnson and Stanier, 1971
DSM 5536	–	**H850**	RefSeq ID: GCF_009663695.2	Isolated from PCB-contaminated soil.	Abbey et al., 2003
DSM 13513	ATCC 43291	**N-1**	RefSeq ID: GCF_000219215.1	Type strain for *C. necator*. Isolated from soil	Poehlein et al., 2011 Makkar and Casida, 1987
DSM 30029	ATCC 25207	**Undefined**	–	Isolate, unable to use H_2 as a source of reducing equivalents	Ertan et al. (2021)
DSM 416	–	LH^{-}7	–	Mutant from H16, negative for soluble hydrogenase	–
DSM 418	–	PH^{-}9	–	Mutant from H16, negative for particulate (membrane) hydrogenase	–
DSM 422	–	PH^{-}4	–	Mutant from H16, negative for particulate (membrane) hydrogenase	–
DSM 430	–	H16 25/1	–	Mutant from H16, requires CO_2 for growth	Ahrens and Schlegel, 1972
DSM 515	–	**B19**	–	Isolated from soil	Gunsalus et al., 1975
DSM 516	–	**G27**	–	Isolated from root region of *Juniperus*	Gunsalus et al., 1975
DSM 517	–	**G29**	–	Isolated from root region of *Juniperus*	Gunsalus et al., 1975
DSM 518	–	**Undefined**	–	Isolated from sludge from a river	Gunsalus et al., 1975
DSM 538 DSM 542 DSM 551	–	H16 G^{+}1 H16 G^{+}7 H16 G^{+}3	–	Mutants from H16, constitutive G-6-PDH expression	Raberg et al., 2011 Schlegel and Gottschalk, 1965
DSM 539 DSM 540	–	H16 F34 H16 F29	–	Mutants from H16, not able to use fructose	Bowien, 1970
DSM 541	–	H16 PHB^{-}4	–	Mutant from H16, does not form PHB	Raberg et al., 2014 Schlegel et al., 1970
DSM 543	–	G29 G^{+}1	–	Mutant from G29, constitutive G-6-PDH expression	König et al., 1969
DSM 544 DSM 547	–	H20 G^{+}3 H20 G^{+}1	–	Mutants from H20, constitutive G-6-PDH expression	Schlegel and Gottschalk, 1965
DSM 545 DSM 546	–	H1 G^{+}3 H1 G^{+}4	–	Mutants from H1, constitutive G-6-PDH expression	König et al., 1969
DSM 2625	–	**1978**	–	Isolated from paddy field soil	Miura et al., 1981
DSM 3102	–	H16 pHS4	–	H16 with additional plasmid pHS4	Schwab et al., 1983
DSM 4182	–	**TA06**	–	Isolated from rhizosphere of *Arum* sp.; unable to use H_2 as a source of reducing equivalents	Jenni et al., 1988
DSM 11098	–	**Tfa 17**	–	Isolated from soil, utilizes tetrahydrofuran-related compound	Zarnt et al., 1997
DSM 13439	–	H850-4LT	–	Engineered from H850 for use of chlorinated benzoates	Wittich and Wolff, 2007
DSM 15443 DSM 15444	–	C145 HF39	–	Mutants from H16	–
–	–	**C39**	RefSeq ID: GCF_016757775.1	Isolated from copper-gold mine in China	Xie et al., 2023
–	–	**UYPR2.512**		Isolated from a root nodule of *Parapiptadenia rigida* in Uruguay	Rodríguez-Esperón et al., 2022 De Meyer et al., 2015
–	–	**SHC 2–3**	RefSeq ID: GCF_013141915.1	Isolated from groundwater in a surface repository of radioactive waste in Russia	–
–	–	**JMP134**	RefSeq ID: GCF_903797845.1	Formerly incorrectly assigned to *C. necator*, currently classified as *C. pinatubonensis*. Noted in RefSeq under strain name "5"	Saraiva et al., 2021 Fetzer et al., 2015 Weightman et al., 1984
–	–	**PHE3–6**	RefSeq ID: GCF_001481455.1 (2015) RefSeq ID: GCF_001853325.1 (2016)	Isolated from soil in Japan	Yonezuka et al., 2016
–	–	**CR12**	RefSeq ID: GCF_003326035.1	Isolated from copper-gold mine in China	–
–	–	**NH9**	RefSeq ID: GCF_002011925.2	Isolated from soil in Japan	Moriuchi et al., 2019
–	–	A5–1	RefSeq ID: GCF_000744095.1	–	–
–	–	**KK10**	RefSeq ID: GCF_018223725.1	Isolated from cattle pasture soil	Mori et al., 2021

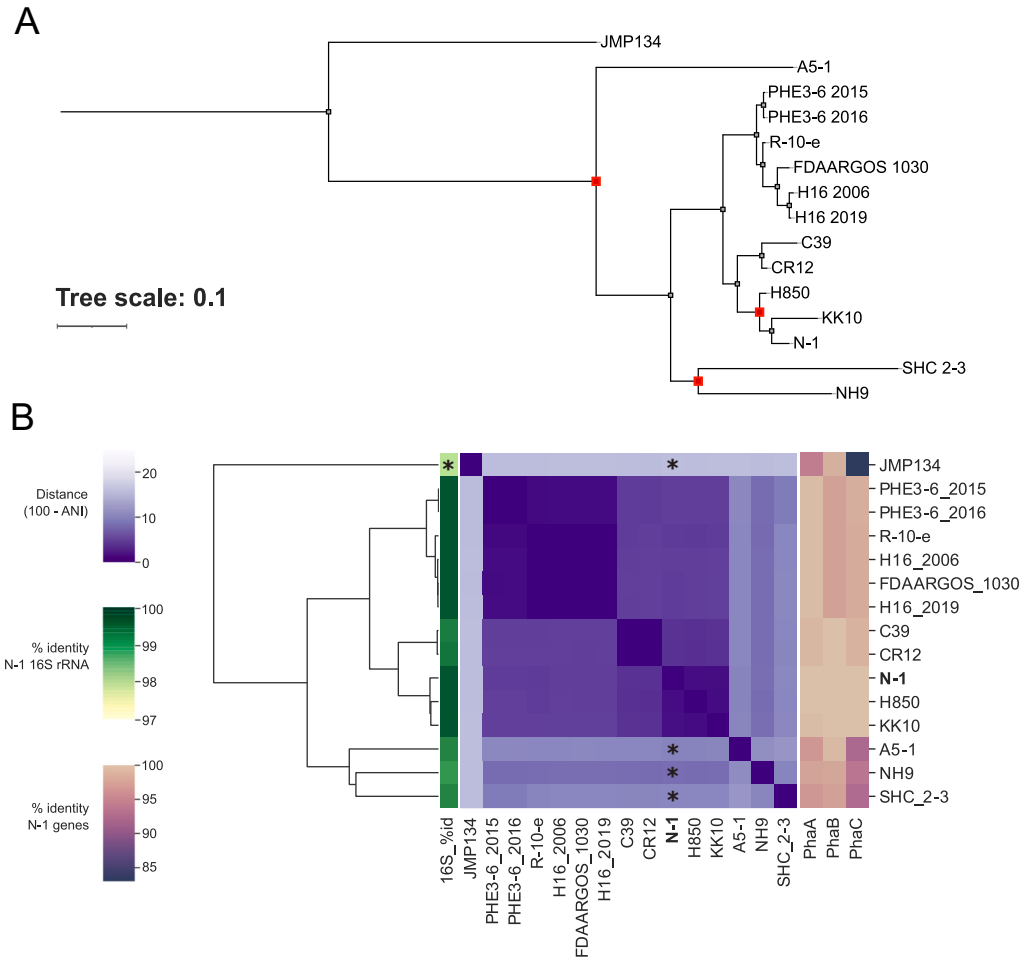

Fig. 1. Phylogeny and genome comparison of *C. necator* strains whose genome sequence is available in RefSeq. (A) Phylogenetic tree inferred from PhyloPhlAn. Nodes with a topology different from (B) are marked in red. Multi-locus sequence analysis was performed with PhyloPhlAn (v. 3.0.67) (Asnicar et al., 2020), which uses conserved genes to inform the construction of the phylogenetic tree. *C. pinatubonensis* JMP134 was selected as an outgroup. (B) Heatmap of genome distances (100 - ANI), dendrogram representing the average linkage clustering of distance values, percent identity of the 16S rRNA region with respect to the type strain, percent identity of proteins PhaCAB with respect to the type strain. 16S percent identity values and ANI values that fall below the thresholds for species assignment are marked with an asterisk. (For interpretation of the references to colour in this figure legend, the reader is referred to the web version of this article.)

HMM was used to search for 16S rRNAs in *C. necator* genomes using the HMMER suite (Wheeler and Eddy, 2013). FASTA sequences of the 16S rRNAs were extracted, a multiple alignment was computed with Clustal Omega (https://www.ebi.ac.uk/Tools/msa/clustalo/), and percentage of identity of each 16S was calculated against the type strain. The topologies of the dendrograms obtained from the two independent methods are in almost complete agreement, with only one discrepancy, observed in the placement of strain A5–1. The most distant strain in the phylogeny is strain JMP134 (BioProject ID: PRJEB38476), wrongly assigned in NCBI as *C. necator*, with the strain name "5" (Saraiva et al., 2021; Fetzer et al., 2015). This strain was classified as *C. necator* in the past, but its current species designation in databases such as BioCyc and the NCBI Taxonomy Browser is in fact *C. pinatubonensis*. It seems that the two designations have conflictually coexisted in the literature between 2010 and 2015. Given the results of ANI and 16S rRNA comparison, JMP134 was considered as outgroup in this analysis. Two genomes are H16 from distinct collections, as is stated in the RefSeq metadata and confirmed by the ANI of over 99.99% (Fig. 1). Finally, strains NH9 and SHC 2–3 have a quite low ANI compared to the type strain, but they are presented in the corresponding papers as *C. necator* nonetheless (Moriuchi et al., 2019). Interestingly, 16S rRNA comparison revealed that all strains apart from JMP134 had a 16S rRNA percent identity of at least 99% with the type strain. Usually, the thresholds employed for species assignment are 95% and 98.5% for ANI and 16S rRNA, respectively (Edgar, 2018; Goris et al., 2007); however, results were not always consistent. For three strains, the 16S rRNA identity was consistent with the species assignment to *C. necator*, while the ANI was substantially lower than the threshold. Moriuchi and collaborators proposed an ANI threshold of 90% instead of 95% for establishing the species assignment to *C. necator*, and remarked that several bacterial species are characterized by non-standard ANI cut-off points (Moriuchi et al., 2019). Notably, ANI and 16S rRNA identity agree for *Cupriavidus* KK10, which in NCBI is not assigned to the species *C. necator*. These observations suggest that the strain should be assigned as *C. necator*. As the ability to synthesize PHA is one of the salient characteristics of *C. necator* as a species of industrial interest, the presence and inter-strain variability of the *phaCAB* operon was also assessed. To do so, the nucleotide sequences of *phaA*, *phaB* and *phaC* genes was searched against each genome with BLAST (Altschul et al., 1990). The coordinates of the best hits were compared to the annotation files to find in each strain the corresponding annotation with its associated RefSeq Protein ID. For each gene, amino acid sequences from RefSeq Protein were aligned with Clustal Omega (https://www.ebi.ac.uk/Tools/msa/clustalo/) and visualized with MView (https://www.ebi.ac.uk/Tools/msa/mview/). Furthermore, the percent identity of each protein to the sequence of the type strain was calculated (Fig. 1). For all three proteins, the active site residues were identical across all examined strains (data not shown). Amino acid sequence was strongly conserved, with a percent identity always >90%,

with the only exception of the PhaC of strain JMP134, which was only 83% identical to the type strain protein. However, it is highly plausible that the function of PHA synthesis is well-conserved across strains under exam. Overall, the results of genome comparisons suggest that some of the current species designations should be corrected. Further analyses on newly released genomes and thorough physiological characterization will acclarate and, possibly, redefine the taxonomy of *C. necator* strains in the future.

According to Pubmed search results, strain H16 is by far the most widely studied and employed in biotechnological applications. Over the years, it has established itself as the most popular chassis not only for PHA production, but for a wide range of platform chemicals and circular economy applications (Sohn et al., 2021; Section 3.2). It is the strain which has been characterized best in terms of metabolic capabilities and cellular physiology. In fact, both GSMMs available for *C. necator* are based off strain H16. The second most frequently mentioned strain, especially regarding PHA production, is DSM 545, a mutant derived from strain H1 expressing constitutive glucose-6-phosphate dehydrogenase (G-6-PDH) (König et al., 1969). Other strains are mentioned in a limited number of manuscripts for specific applications, often related to bioremediation or degradation of recalcitrant polluting compounds (Table 1).

Notably, very few research has been conducted to directly compare metabolic capabilities and PHA yields of different strains. For many strains, it has not been experimentally validated whether they are facultative anaerobes and facultative autotrophs like strain H16. Where the genome sequence is available, it is possible to assess the presence of the genes related to the different metabolic lifestyles. This has been done for strain N-1, the *C. necator* type strain, in which genes for hydrogen oxidation, necessary to grow in chemolithotrophy, were not detected (Poehlein et al., 2011). Most genome sequences have high levels of identity (> 98%) to either strain H16 or strain N-1 (Fig. 1). It is likely that these highly similar groups of strains share similar physiological characteristics, though this needs to be verified firstly by checking the presence of specific genes, secondly experimentally. Strains with lower identity to well-characterized counterparts are either not yet characterized (A5–1, CR12, SHC 2–3), or the analysis of their genomic sequences was focused on genes for the degradation of aromatic compounds (NH9, Moriuchi et al., 2019) or resistance to metals (C39, Xie et al., 2023). Thus, the physiological characteristics of *C. necator* as described in the following section mainly regard *C. necator* H16.

3. Overview of *C. necator* metabolism

3.1. Electron donors and acceptors

The metabolism of *C. necator* is extremely versatile. The strain which has been best characterized and displays the most variable physiological behaviors is *C. necator* H16. The metabolic paradigms of this strain can be easily summarized by considering the electron donors and electron acceptors that it can utilize for energy conservation, and whether the carbon source is organic or inorganic. *C. necator* H16 can utilize either reduced organic compounds or hydrogen as electron donors, leading to heterotrophic or chemolithotrophic lifestyles, respectively. In heterotrophic metabolism, the reduced organic compounds serve as carbon source, while chemolithotrophic metabolism relies on 1-carbon molecules. In particular, in *C. necator* H16, chemolithotrophy can occur with CO_2 or formate as carbon sources. Mixotrophy has also been observed, and it has been shown that it can even aid growth when utilization of a reduced organic carbon source is inefficient (Jawed et al., 2022; Strittmatter et al., 2022; Alagesan et al., 2018). The final electron acceptor is oxygen for aerobic growth, but the bacterium is also able to perform anaerobic respiration by reducing nitrate via a complete denitrification pathway (Pohlmann et al., 2006).

Heterotrophic growth can occur in several strains with a variety of organic carbon sources, including fructose, *N*-acetyl-glucosamine, gluconate, PHA precursors and derivatives (e.g. caproic acid, 3-hydroxybutyrate), amino acids, tricarboxylic acid cycle (TCA) intermediates, and volatile fatty acids (VFA) (Jawed et al., 2022; Pearcy et al., 2022; Sohn et al., 2021; Schlegel et al., 1961). A comprehensive list of viable substrates in wild-type *C. necator* H16 is reported in Pearcy et al., 2022. In the case of fructose metabolism, fructose uptaken by the cell is converted to glucose-6-phosphate, which enables it to enter the Entner-Doudoroff (ED) pathway. The key enzyme for the more efficient Embden-Meyerhof-Parnas (EMP) pathway, phosphofructokinase, is not encoded in H16's genome (Raberg et al., 2011; Pohlmann et al., 2006). Despite this, the rest of the pathway is encoded, including the key enzyme of gluconeogenesis, allowing for glucose synthesis when carbon sources are simpler organic or inorganic molecules. The pyruvate generated by sugar degradation is oxidized to acetyl-CoA and enters the TCA to be heterotrophically respired to CO_2. The reduced cofactors generated by the ED and TCA pathways carry electrons to the respiratory chain, with O_2 as final electron acceptor (Fig. 2). In particular, NADH is generated by the ED pathway, and reduced ubiquinones are generated by succinate dehydrogenase in the TCA. NADPH, whose primary role is to provide electrons for anabolic reactions, is frequently generated from $NADP^+$ reduction via pentose phosphate pathway (PPP) in prokaryotes (Spaans et al., 2015). However, the key enzyme of this route, 6-phosphogluconate dehydrogenase, is lacking in *C. necator* H16. Thus, $NADP^+$/NADPH balance is maintained by the isocitrate dehydrogenase reaction in the TCA cycle. Additionally, the pools of NADH and NADPH are balanced by membrane-bound transhydrogenase PntAB, which couples transfer of a hydride ion from NADH to $NADP^+$ with proton translocation (Raberg et al., 2011; Cramm, 2009; Sauer et al., 2004, Fig. 2). The transhydrogenase reaction is reversible, and although its activity in the direction of NAD^+ reduction has not been reported specifically in *C. necator* H16, it may occur in situations where it is necessary to feed the respiratory chain.

Notably, *C. necator* H16 is not able to grow on glucose. The most plausible reason for this inability is the lack of a transport system for glucose intake (Raberg et al., 2011). Mutants with the ability to grow on glucose were obtained a few years after the first isolations via UV-ray exposure (Raberg et al., 2011; König et al., 1969; König, 1967; Schlegel and Gottschalk, 1965). A multiomic study proved that in the mutant strain H16 G^+1, glucose uptake is enabled by transcriptional derepression and point mutations in the transporter for *N*-acetyl-glucosamine. The mutated transporter has sufficient affinity for glucose and allows its uptake. In turn, glucose availability upregulates ED pathway enzyme glucose-6-phosphate-dehydrogenase (G-6-PDH) (Raberg et al., 2011). It is likely that other glucose-utilizing mutants, which are often labeled as "G^+" in DSMZ, acquired the capacity of importing glucose in the cell through a similar mechanism. Indeed, constitutive G-6-PDH expression is reported for all "G^+" mutants in DSMZ, including the most popular glucose-utilizing strain, DSM 545 (Table 1).

In the chemolithotrophic lifestyle, energy conservation occurs via oxidation of hydrogen. *C. necator* H16 is endowed with a soluble hydrogenase (SH) and a membrane-bound hydrogenase (MBH). Both are Ni—Fe hydrogenases, and the soluble form contains cyanide groups that confer tolerance to oxygen (Cramm, 2009; Van der Linden et al., 2004). MBH faces the periplasm and feeds electrons directly into the respiratory chain, but its reduction potential is higher than that of $NAD(P)^+$. Conversely, SH is able to reduce $NAD(P)^+$ and create reducing equivalents for anabolic pathways, including carbon fixation (Bowien and Schlegel, 1981). Remarkably, production of reducing equivalents through SH allows to bypass the process of reverse electron flow, which has the same purpose in bacteria which cannot reduce $NAD(P)^+$ directly. Expression of SH and MBH is controlled by a regulatory hydrogenase which acts as a hydrogen sensor (Lenz et al., 2002). Carbon is fixed via the Calvin-Benson-Bassham (CBB) pathway, with RuBisCO as the key enzyme. *C. necator* H16 has been grown successfully with CO_2 concentrations of 10–20%. Growth at low CO_2 concentrations, such as those found in the atmosphere (currently about 400 ppm, i.e., 0,04%) is also

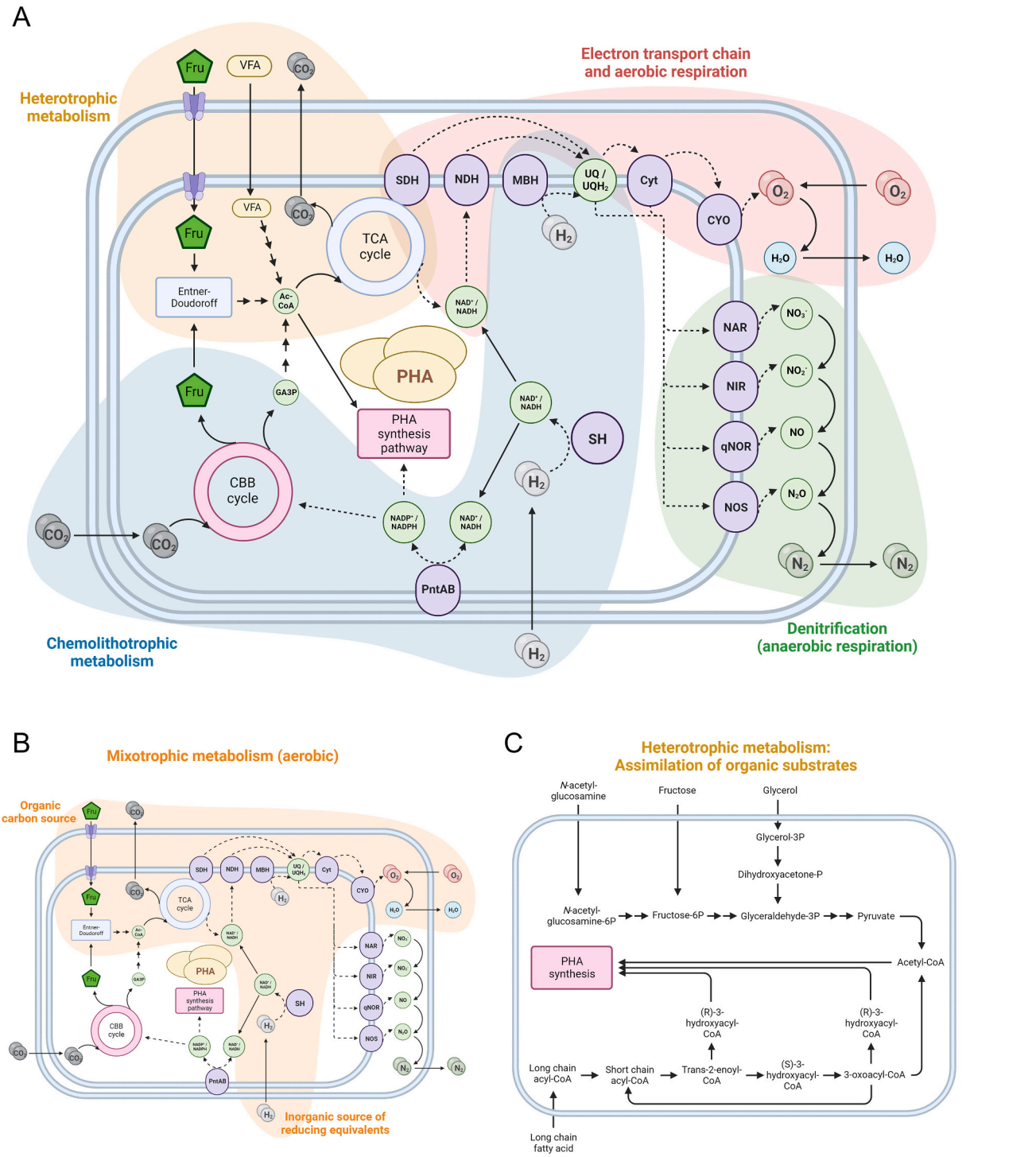

Fig. 2. Overview of metabolic paradigms and main pathways in *C. necator*. (A) Schematic representation of the core carbon and energy metabolism of *C. necator*. Electron flows are represented with dotted arrows, metabolite/carbon flows with solid arrows. Violet elements are oxidoreductases, light blue are catabolic pathways, red are anabolic pathways. Abbreviations and gene symbols used in this figure: Fru, fructose; Ac-CoA, acetyl-coenzyme A; TCA, tricarboxylic acid; SDH, succinate dehydrogenase; SH, soluble hydrogenase; MBH, membrane-bound hydrogenase; PntAB, transhydrogenase; CBB, Calvin-Benson-Bassham; GA3P, glyceraldehyde-3-phosphate; NDH, NADH dehydrogenase; UQ, ubiquinone, Cyt, b/c-type cytochrome; CYO, cytochrome oxidase; NAR, nitrate reductase; NIR, nitrite reductase; NOR, nitric oxide reductase; NOS, nitrous oxide reductase. (B) Highlight on pathways involved in mixotrophic metabolism. (C) Pathways of assimilation and conversion to PHA of distinct carbon sources in wild-type *C. necator*. Created with BioRender.com. (For interpretation of the references to colour in this figure legend, the reader is referred to the web version of this article.)

possible, but requires the activity of carbonic anhydrase Can, encoded in chromosome 1, catalyzing the conversion of bicarbonate to CO_2 to support growth (Kusian et al., 2002). Interestingly, *C. necator* H16 encodes three more carbonic anhydrases, for which distinct roles have been proposed, including conversion of CO_2 to bicarbonate to avoid its rediffusion outside of the cell, reconversion of bicarbonate to CO_2 to supply to the CBB cycle, and CO_2-bicarbonate interconversion to maintain pH (Gai et al., 2014). In addition to CO_2, *C. necator* has the

ability to use formate as carbon source, which is first oxidized to CO_2 by a soluble formate dehydrogenase, with the concomitant reduction of NAD^+, and then enters the CBB cycle as such.

By definition, mixotrophy occurs when organic carbon and reducing equivalents are obtained by different substrates: for example, an organic compound can be assimilated and used for anabolic pathways instead of being respired, while energy is conserved chemolithotrophically by H_2 oxidation. Mixotrophy has been observed in *C. necator* H16 growing with organic substrates, such as VFA, that are used by the organism with limited efficiency (Strittmatter et al., 2022). Additionally, there is evidence of CBB activity during growth on sugars, with recapturing of the CO_2 obtained through respiration. Fluxomic data and flux balance analysis (FBA) simulations on metabolic models lend themselves to multiple interpretations: some researchers propose that this activity confers an evolutionary advantage as it optimizes carbon utilization; others find no evidence of such advantage, suggesting instead that synthesizing excess CBB enzymes is an investment in order for the organism to readily switch to chemolithotrophic metabolism when needed (Pearcy et al., 2022; Jahn et al., 2021; Shimizu et al., 2015).

Anaerobic growth is enabled in *C. necator* H16 by a specialized respiratory chain that covers the whole denitrification pathway, reducing nitrate to molecular nitrogen in four steps and using each intermediate as terminal electron acceptor (Kohlmann et al., 2014; Pfitzner and Schlegel, 1973; Fig. 2). Although it has been observed in heterotrophic conditions, it is very limited with hydrogen and CO_2 as the only substrates, with limited research available (Kohlmann et al., 2014; Pfitzner and Schlegel, 1973). All enzymes for denitrification except for nitrite reductase are encoded in megaplasmid pHG1. Dissimilatory reduction of nitrate to nitrite is carried out by molybdopterin-containing nitrate reductases NAR and NAP. Both are membrane-bound and their catalytic subunits face the cytoplasm and periplasm respectively. Biochemical characterization of both enzymes in *C. necator* H16 is partial, however it is known that they are involved in anaerobic respiration and use quinol as the electron donor. NAR genes are encoded in megaplasmid pHG1 and their expression is likely regulated by nitrite and nitrate concentration, while NAP genes are encoded in chromosome 2 and expressed during the stationary growth phase (Cramm, 2009; Schwartz et al., 2003; Siddiqui et al., 1993). A study evaluating transcriptomic and proteomic changes in anaerobic conditions evidenced the marginal role of NAP in acclimation to anaerobiosis, while NAR activity is more prominent (Kohlmann et al., 2014). The denitrification pathway continues with the reduction of nitrite to nitric oxide by heme-containing nitrite reductase (NIR) enzyme, which is encoded in chromosome 2. Subsequently, nitric oxide is reduced to nitrous oxide by nitric oxide reductase (NOR), which again receives electrons from quinol for the reaction (Cramm, 2009; Cramm et al., 1999). Finally, nitrous oxide is reduced to molecular nitrogen by NOS, whose putative electron donor is a *c*-type cytochrome (Cramm, 2009). Interestingly, adaptation to anaerobiosis is associated with changes in enzymes with a role in redox balancing mechanisms: anoxic conditions lead to the derepression of NAD-linked enzymes such as lactate dehydrogenase and alcohol dehydrogenase, while the NADPH pool is sharply diminished via a limited activity of transhydrogenase PntAB and NAD^+ kinase (Kohlmann et al., 2014; Cramm, 2009).

The different lifestyles of *C. necator* can be used to convert a wide array of substrates to biomass and PHA. Anaerobic growth is characterized by a long lag phase and a limited biomass productivity, so it is generally not explored for large-scale applications (Pfitzner and Schlegel, 1973). In aerobiosis, chemolithotrophic and heterotrophic metabolisms have similar biomass yields, and experimental data prove that theoretical yields dictated by stoichiometry are attainable (Unrean et al., 2019; Ishizaki and Tanaka, 1990). However, the most convenient lifestyle depends on the application of choice: heterotrophic growth proves more advantageous when employing batch mode cultivations, where the only limiting factor is oxygen availability, while chemolithotrophic growth rate is heavily dependent on gas-liquid mass transfer, and therefore requires an accurate choice of bioreactor configurations and operational parameters to be cost-effective (Miyahara et al., 2022). A more detailed description of productivities and yields in different lifestyles is given in Section 4.

3.2. PHAs: structure, functions, and biosynthetic pathways

Polyhydroxyalkanoates (PHA) are a class of polymers synthesized by several bacterial and archaeal genera (Koller et al., 2013; Lemoigne, 1926). Their chemical structure involves a main chain with ester bonds, where the γ carbon of each repetitive unit harbors a side chain that depends on the monomers used by the organisms for synthesis and determines the specific type of PHA (Fig. 3). Many biologically produced PHAs are optically active, specifically those where the building blocks are 3-hydroxyalkanoates. Notably, the enzyme PHA synthase, which catalyzes polymerization, has a specificity for R(−)-3hydroxyalkanoates (Kessler and Witholt, 1998). The most common PHA is poly(3-hydroxybutyrate) (P[3HB], or PHB), where the monomeric building block is 3-hydroxybutyrate (3HB). This polymer is naturally synthesized in high concentrations by *C. necator*. Other biologically generated PHAs are generally classified based on the chain lengths. Namely, 3-hydroxybutyrate and 3-hydroxyvalerate are classified as short chain length monomers, while longer monomers, up to 3-hydroxytetradecanoate, fall into the medium chain length category (Koller, 2019; Laycock et al., 2014; Steinbüchel et al., 1992). Very few PHAs, including PHB, occur as homopolymers. Most copolymers are random copolymers, although biological block co-polymer synthesis has been achieved through targeted feeding strategies (Chen, 2010; Fig. 3). The physical, chemical, and mechanical properties of PHA heavily influence the applicability in downstream processes. The most relevant physical properties for industrial PHA production are melting temperature, crystallization rate, melt stability, tensile strength, and maximum elongation to break. Such properties are influenced by the type, percentage and distribution of monomers incorporated in the polymer, and can thus be tweaked to some extent to fit the suitability to different applications (Laycock et al., 2014; Sudesh et al., 2000). The most popular random copolymer for industrial applications is poly(3-hydroxybutyrate-*co*-3-hydroxyvalerate) (P[HB-co-HV], or PHBV) (Rivera-Briso and Serrano-Aroca, 2018). This copolymer is often obtained in bioprocesses utilizing feedstocks containing propionic acid, which can be condensed with acetate to yield 3-hydroxyvalerate (3HV), and subsequently incorporated by the PHA synthase of wild-type *C. necator* (Byrom, 1987). The presence of 3HV moieties introduces irregularities in the crystal structure, yielding a less brittle material than pure PHB; in addition, the melting temperature is lower, widening the range of temperatures in which the polymer can be processed (de Koning, 1995). Another polymer, poly(4-hydroxybutyrate) (P[4HB]), is the only PHA approved by FDA for medical applications, as 4HB is a metabolite normally present in the human body, resulting in a non-toxic, low-impact material for implants, mesh, and drug delivery devices (Utsunomia et al., 2020; Zhang et al., 2018). While PHAs have great potential to become substitutes of petroleum-based plastics, most of them are obtained through bioprocesses with low productivities and yields, or require the use of additives and plasticizers for processing, as well as long processing cycle times (Rivera-Briso and Serrano-Aroca, 2018; Kourmentza et al., 2017; de Koning, 1995). These factors should be evaluated carefully in life cycle and sustainability assessments. Nevertheless, the biochemical aspects of PHA synthesis have been researched extensively. The rest of the paragraph proceeds to summarize them, focusing on biological PHB production in *C. necator*.

Pathways for PHA production have been studied in bacterial genera such as *Cupriavidus*, *Pseudomonas*, and *Clostridium* (Meng et al., 2014). Building blocks for PHAs are generated from precursor molecules such as fatty acids, TCA intermediates, and acetyl-CoA. All pathways have a step which involves PHA synthase. The composition of the biopolymer can vary based on the specific pathway and the carbon source, as well as the specificity of PHA synthase for particular side chain lengths (Meng

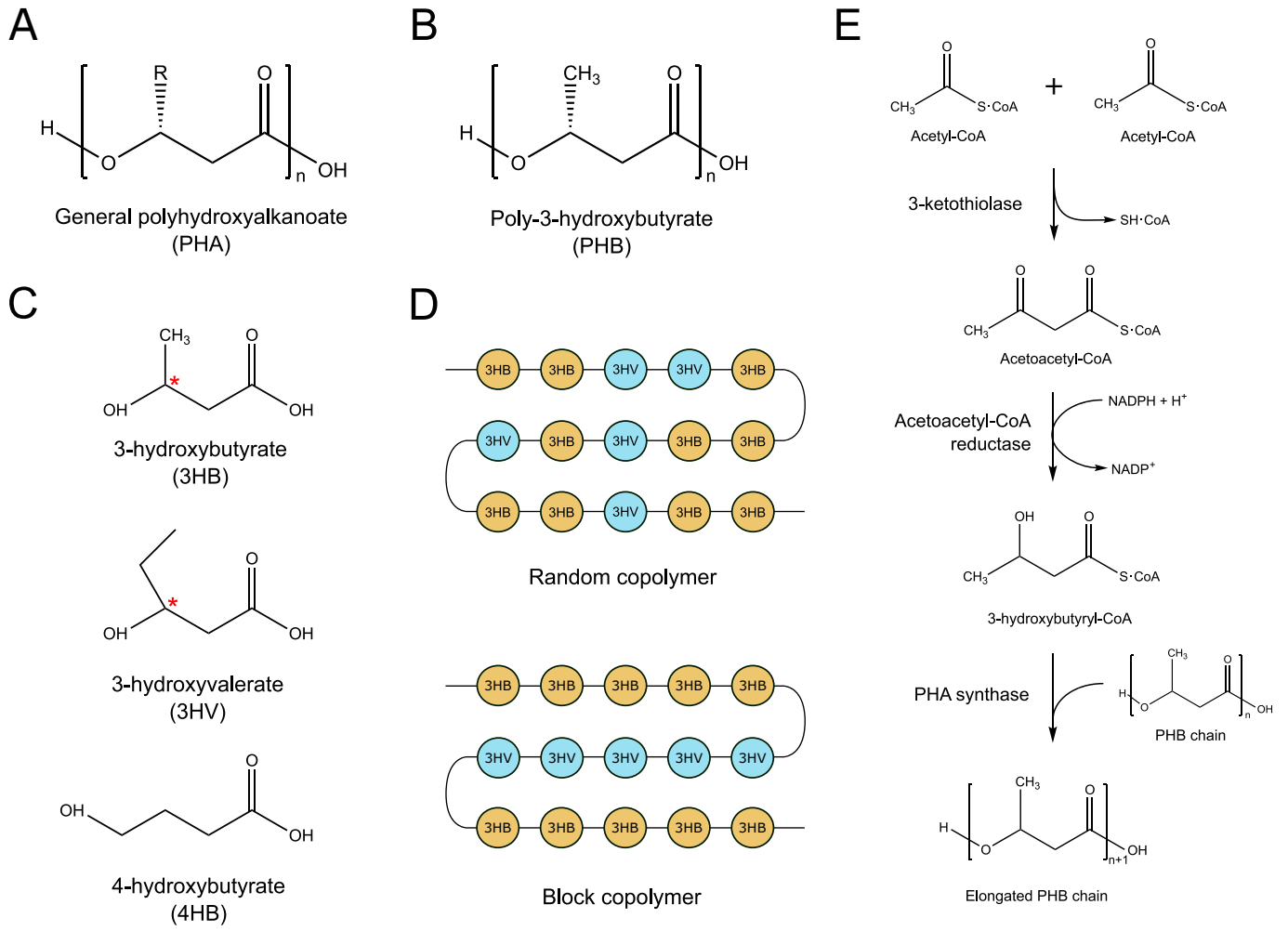

Fig. 3. Overview of PHAs. A. General chemical structure of poly-3-hydroxyalkanoates. B. Chemical structure of poly-3-hydroxybutyrate (P[3HB]). C. Chemical structure of relevant monomers. Chiral carbons are marked with a red asterisk. D. Schematic representation of PHBV random copolymers versus block copolymers. E. Pathway for P(3HB) production in *C. necator*. (For interpretation of the references to colour in this figure legend, the reader is referred to the web version of this article.)

et al., 2014). All strains of *C. necator* are endowed with a class I PHA synthase, which has a preference for short-chain monomers, usually up to 5 or 6 carbon atoms (Koller, 2019). Biologically, PHA synthesis serves to accumulate carbon reservoirs when carbon source is abundant and other nutrients, such as nitrogen, phosphates, and sulfur, are not. It also covers an important role in maintaining the redox balance of the cell, which is why it is often linked to stressful growth conditions. Indeed, PHA synthesis normally occurs to a limited extent, and it is enhanced when the cell accumulates a high energy charge (Koller et al., 2013; Castro-Sowinski et al., 2010; Schlegel et al., 1961). This condition is favored by nutrient depletion, as reduced cofactors accumulate in the cell and saturate electron transport chains. This over-reduction can lead to the formation of reactive oxygen species and free radicals, which are deleterious to the cell (Rochaix, 2011). Thus, PHA synthesis provides a sink for the accumulation of NAD(P)H and acetyl-CoA, allowing to replenish the pool of oxidized cofactors and free CoA. In this sense, as *C. necator* is a strictly respiratory organism (i.e., not performing fermentation), it utilizes PHA synthesis as a pseudo-fermentative pathway (Koller et al., 2013). Additionally, many studies suggest that in some bacterial species, PHA synthesis is initiated when environmental stresses arise, for example UV irradiation, heat and osmotic shock, desiccation, and oxidative stress (Castro-Sowinski et al., 2010). In *C. necator* H16, the presence of PHA granules was found to be associated with the maintenance of cellular viability in presence of these shocks, suggesting a protective role against stresses (Koller, 2019). As previously discussed, in case of external factors limiting growth, PHA enables storing excess reducing power, avoiding the risks from over-reduction. An interesting experimental observation is that even when metabolic conditions favor PHA accumulation, the pathways of PHA synthesis and degradation are simultaneously active (Doi et al., 1990). The mechanism of PHA recycling, dubbed PHA cycle, is corroborated by experimental data and FBA simulations, and it likely has a role in the maintenance of redox balance (Pearcy et al., 2022; Doi et al., 1990). Furthermore, roles of the PHA cycle have been investigated in several bacterial species, demonstrating that availability of free 3HB in the cell may protect from protein denaturation by high temperature, high salt concentrations, osmotic pressure, and oxidative stress (Koller, 2019; Obruca et al., 2020).

The pathway for PHB production in *C. necator* consists of three steps. In the first step, two molecules of acetyl-CoA are condensed by 3-ketothiolase to form acetoacetyl-CoA (PhaA). In the second step, acetoacetyl-CoA reductase (PhaB) converts the metabolite into 3-hydroxybutyryl-CoA, with consumption of NADPH. Finally, the molecule is added to an existing polymer by PHA synthase (PhaC) (Peoples and Sinskey, 1989a; Peoples and Sinskey, 1989b; Schubert et al., 1988; Fig. 3). The genes participating in the pathway are organized in a single operon named *phaCAB*. Nucleotide sequence and function are strongly conserved in several bacterial families able to synthesize PHB, and

across *C. necator* strains (Reddy et al., 2003). In this canonical pathway, the central metabolite and precursor to PHB synthesis is acetyl-CoA. This key metabolite links most pathways related to central carbon metabolism, such as the TCA, beta-oxidation pathway, fatty acid synthesis, and glyoxylate shunt. In particular, the rate of PHB synthesis is finely balanced against TCA activity, based on whether the flux of acetyl-CoA is directed towards the TCA or towards the condensation reaction catalyzed by PhaA (Sun et al., 2020). In particular, TCA enzymes citrate synthase and isocitrate dehydrogenase are allosterically inhibited by high acetyl-CoA and NAD(*P*)H levels (Koller et al., 2013). These high-energy metabolites accumulate when the carbon source is available, but biosynthesis of other molecules (i.e., proteins, amino acids, nucleic acids, cofactors) is impaired by the lack of key nutrients such as nitrogen or phosphate (Koller et al., 2013). Aside from nitrogen and phosphate limitation, PHB synthesis can be elicited by oxygen depletion. This stress was found to be particularly effective in chemolithotrophic conditions, as the reducing equivalents generated by the consumption of hydrogen cannot be exhausted in oxygen reduction and are thus redirected to PHB synthesis and can be even applied in combination with nitrogen limitation (Mozumder et al., 2015). As anticipated in Section 1, the dramatic increase in CO_2 atmospheric concentration caused by human activities has raised particular interest in chemolithotrophic PHA production, as a means to sequester CO_2 in the medium-long term. Hence, research on CO_2 to PHA bioconversion will be fundamental in the near future.

4. Carbon-rich waste streams for PHA production

The ability of *C. necator* to synthesize PHAs with high productivity and yields in optimal culturing conditions has been noted early on after its isolation (Ishizaki and Tanaka, 1991; Doi et al., 1990; Schlegel et al., 1961). As noted in Section 3.2, PHA is endowed with mechanical characteristics similar to other petroleum-based plastics, e.g., polypropylene (Dalton et al., 2022). The substitution of the latter by PHAs would allow for mass production of disposable objects without consumption of non-renewable resources. In addition, PHA is entirely biodegradable and biocompatible, as long as the monomers are not chemically altered. Thus, the positive environmental impact of PHA with respect to petroleum-based plastic is manifold: on one hand, it allows to limit the consumption of petrol deposits, which act as important carbon reservoirs in the global carbon cycle; on the other hand, the superior biodegradability of PHA and the biocompatibility of its monomers would alleviate the problem of the accumulation of plastic waste and the capillary diffusion of potentially damaging microplastic particles in the environment (Amobonye et al., 2021). However, PHA production is a slow and costly process, heavily impacted by the carbon source used for microorganism growth and bioconversion. The feedstock of choice was estimated to affect the final cost of PHA for up to 50% (Dalton et al., 2022; Nonato et al., 2001). As economic feasibility is a key factor to successfully introduce and promote large-scale PHA production, research efforts were spent over the past decades towards the utilization of carbon-rich waste streams as feedstocks, in order to drastically reduce the costs (Sohn et al., 2021). This strategy is rooted in the framework of circular economy, which attempts to establish loops where the byproducts of industrial processes are reused as input to other processes. Therefore, waste release in the environment is delayed, and resource utilization is optimized (Geissdoerfer et al., 2017). Waste streams suitable for utilization in this scenario have a high amount of residual carbon, which can be uptaken by the microorganisms. This carbon mainly comes in the form of organic molecules, such as sugars, cellulose, lignocellulose, VFA, etc.. This is the case for waste streams such as cheese whey from the dairy industry, sugar-rich molasses derived from beet processing, and cellulose- and starch-rich agricultural crops. Even glycerol, which is generated as a byproduct of biodiesel production, can be metabolized by *C. necator*, and therefore is suitable as a substrate for bioconversion to PHA (Fig. 4). Importantly, a potential carbon source is the CO_2 present in gaseous waste streams, such as combustion products and syngas. Valorization of CO_2-rich waste streams is especially relevant as it prevents CO_2 from being released in the atmosphere, allowing to cut down emissions from other industrial activities (Fig. 4, Section 4.2).

4.1. Organic waste streams

As anticipated in the previous section, wild-type *C. necator* is able to grow heterotrophically using a wide range of substrates, among which glycerol, VFA and sugars have been investigated in detail (Table 2).

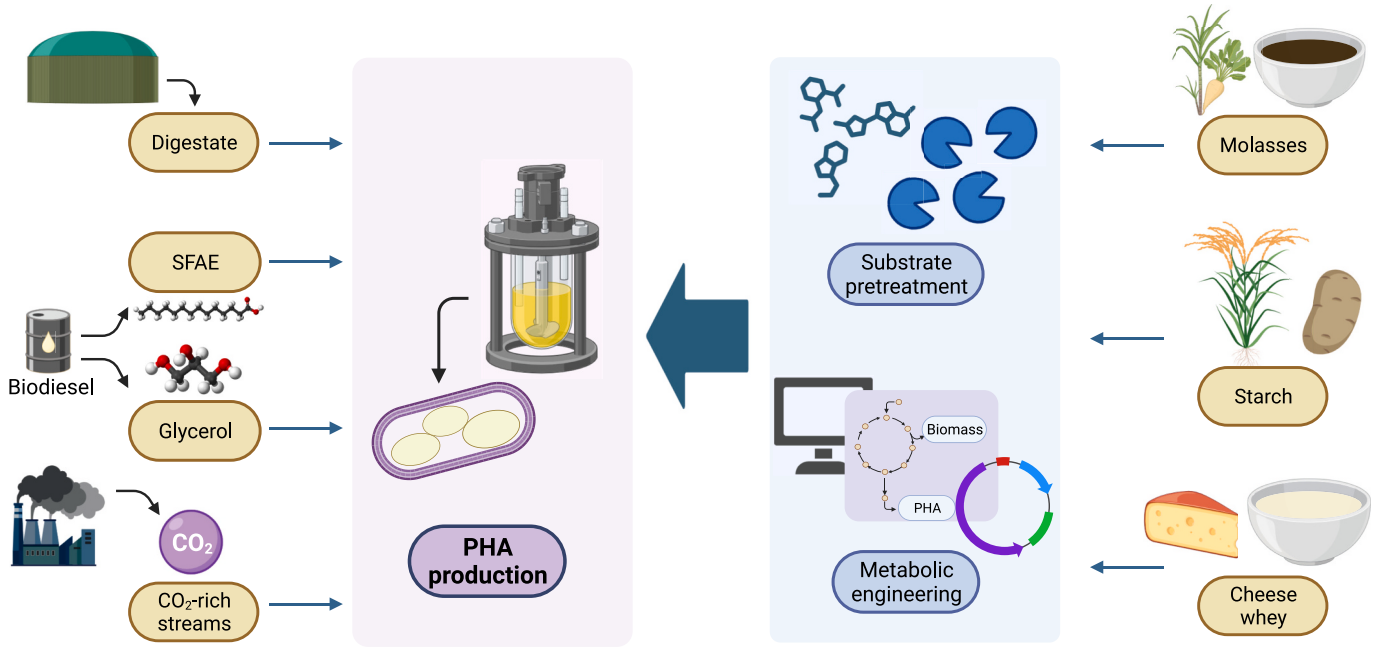

Fig. 4. Waste streams that can be employed as carbon sources for PHA production. Possible substrates that can be utilized by *C. necator* are represented, divided according to substrates that can be used directly and substrates that need pretreatments and/or metabolic engineering approaches. Created with BioRender.com.

Table 2
PHA production from waste materials and different *C. necator* strains, including isolates, mutants, and engineered strains.

Carbon source	Strain	Strain features	PHA/substrate yield (g/g)	PHA content (%)	PHA productivity (g/(L·h))	Reference
Glycerol	DSM 545	Ability to use glucose	–	70.9	–	Špoljarić et al. (2013)
SFAE	DSM 545	Ability to use glucose	0.65	–	0.98	Koller and Braunegg (2015)
CGP	DSM 545	Ability to use glucose	0.60	–	0.95	Koller and Braunegg (2015)
Valerate	H16	Wild type	–	10.2	–	Jawed et al. (2022)
Artificial VFA mixture plus CO_2 and H_2	H16	Wild type	–	57.0	–	Jawed et al. (2022)
VFA from digestate	H16	Wild type	–	1.3–53.6	–	Jawed et al. (2022)
Non-hydrolyzed whey permeate	DSM 545 mRePT	Gene *phaZ* disrupted by insertion of *lac* operon from *E. coli*	–	30.0	–	Povolo et al. (2010)
Hydrolyzed whey permeate	DSM 545 mRePT	Gene *phaZ* disrupted by insertion of *lac* operon from *E. coli*	–	22.0	–	Povolo et al. (2010)
Soluble potato starch	DSM 545 (recombinant)	Co-expression of heterologous glucodextranase and *alpha*-amylase	0.19	61.6	–	Brojanigo et al. (2022)
Broken rice	DSM 545 (recombinant)	Co-expression of heterologous glucodextranase and *alpha*-amylase	0.19	43.3	–	Brojanigo et al. (2022)
Purple sweet potato waste	DSM 545 (recombinant)	Co-expression of heterologous glucodextranase and *alpha*-amylase	0.12	36.0	–	Brojanigo et al. (2022)
Raw corn starch	DSM 545 (recombinant)	Co-expression of heterologous glucodextranase and *alpha*-amylase	0.20	48.2	–	Brojanigo et al. (2022)
Ground date seeds	H16	Wild type	0.26–0.46	73.0–75.0	–	Yousuf and Winterburn (2016)
Date seed oil	H16 Re 2085/pCB113	Substitution of endogenous *phaC1* and *proC* with heterologous *phaC2*, *phaJ*, and *proC*	0.62	81.0	–	Purama et al. (2018)
Date molasses	H16 Re 2085/pCB113	Substitution of endogenous *phaC1* and *proC* with heterologous *phaC2*, *phaJ*, and *proC*	0.07	32.0	–	Purama et al. (2018)
Enzymatically hydrolyzed chicory roots	H16	Wild type	0.32	66.0	0.062	Haas et al. (2015)
Enzymatically hydrolyzed chicory roots	DSM 545	Ability to use glucose	0.38	78.0	0.15	Haas et al. (2015)
Enzymatically hydrolyzed chicory roots	DSM 531	Wild type	0.15	46.0	0.016	Haas et al. (2015)
Acid-treated beet molasses	ATCC 25207	Wild type	0.5	52.9	0.33	Ertan et al. (2021)
Hydrothermal acid pretreated cane molasses	Not specified	–	0.078	27.3	0.013	Sen et al. (2019)
Cane and beet molasses	DSM 545	Ability to use glucose	0.06	1.1	–	Baei et al. (2011)
Vinasse and enzyme-digested sugarcane molasses	DSM 545	Ability to use glucose	–	56.0	–	Dalsasso et al. (2019)
Sugar beet molasse hydrolysates	B-10646	Wild type	–	77.0–80.0	–	Kiselev et al. (2022)
Charcoal-treated sugarcane molasses	NCIMB 11599 (recombinant)	Expression of heterologous *sacC* gene	–	82.5	–	Jo et al. (2021)
Purified glycerol	IPB/SFU-1	Wild type. Ability to utilize glucose	0.29	65.1	0.045	Zhila et al. (2021)
Palm oil	IPB/SFU-1	Wild type. Ability to utilize glucose	0.48	80.0	0.114	Zhila et al. (2021)
Sunflower seed oil	IPB/SFU-1	Wild type. Ability to utilize glucose	0.48	38.7	0.073	Zhila et al. (2021)
H_2:CO_2:O_2	IPB/SFU-1	Wild type. Ability to utilize glucose	–	35.1	–	Zhila et al. (2021)
H_2:CO_2:O_2 = 75:10:15	H16	Wild type	–	60.0	–	Ishizaki and Tanaka (1991)
H_2:CO_2:O_2 = 75:10:15	H16	Wild type	–	67.0	–	Tanaka et al. (1995)
H_2:CO_2:O_2 = 75:10:15	H16	Wild type	–	82.0	–	Taga et al. (1997)
H_2:CO_2:O_2 = 85:10:2	H16	Wild type	–	79.0	–	Lambauer and Kratzer (2022)

(*continued on next page*)

Table 2 (*continued*)

Carbon source	Strain	Strain features	PHA/substrate yield (g/g)	PHA content (%)	PHA productivity (g/(L·h))	Reference
H_2:CO_2:O_2 = 70:10:2.5	H16 (recombinant)	Expression of heterologous *vgb*, knockout of *ldh*	–	50.4	–	Tang et al. (2020)
H_2:CO_2:O_2 = 80:10:10	MF01 (H16 recombinant)	Substitution of wild-type *phaA* and *phaC* with heterologous *bktB* and $phaC_{NSDG}$ with specificity for longer monomers; insertion of heterologous genes ccr_{Me}, *phaJ4a*, and emd_{Mm}	–	85.8	–	Tanaka et al. (2021)
Model gas mixtures mimicking syngas, with 10–20% CO	B5786	Wild type	–	72.8–76.8	–	Volova et al. (2002)
H_2:CO_2:O_2:CO = 20:20:20:40	H16	Wild type, bound to cellulose particles displaying enzymes CooS, CooA, CA for CO reduction	–	42.0	–	Shin et al. (2021)
H_2:CO_2:N_2:CO = 40:10:10:40	H16 (recombinant)	Expression of heterologous *cox* gene cluster for CO uptake	–	49.7	–	Heinrich et al. (2018)

Glycerol is the main by-product from biodiesel production and constitutes a potential carbon substrate for PHA production. However, the growth rate and PHA yield of *C. necator* fed with glycerol are lower compared to more favorable substrates such as fructose or gluconate (Cavalheiro et al., 2009). In silico optimization of biomass and PHA formation in *C. necator* DSM 545 grown on glycerol was studied (Špoljarić et al., 2013) and higher biomass and PHA yields were reported when increasing the initial inoculum biomass. Growth was optimal when glycerol concentration was kept between 5 and 30 g/L, to ensure substrate availability while avoiding inhibition. To elicit PHA accumulation, nitrogen was supplied in very limited quantities. A slower growth than on glucose was observed, while PHA yields were similar or slightly lower. Koller and Braunegg (2015) investigated the biomass and PHA formation by *C. necator* DSM 545 using lipid-rich streams from slaughterhouses. Two fractions from animal-based biodiesel production were compared: saturated share of biodiesel (SFAE) and crude glycerol phase (CGP). The yield and PHA volumetric productivity with CGP were 0.65 g/g and 0.98 g/(L·h), respectively. When using SFAE, these values reached 0.6 g/g and 0.95 g/(L·h). These are promising yields compared to the ones achieved with expensive substrates considering, for instance, that the theoretical yields for sugar do not exceed 0.48 g/g. This work showcased the production of distinct types of PHAs using different substrates: PHBV was produced when using SFAE, while PHB was produced when using CGP. To improve glycerol assimilation, adaptive evolution of *C. necator* has been used. One work involving *C. necator* H16 identified and characterized a variant strain called v6C6 (González-Villanueva et al., 2019). This strain exhibited a 9.5-fold increase in growth rate and the ability to co-utilize both gluconate and glycerol. While wild-type *C. necator* H16 produced more PHA from gluconate than from glycerol, variant v6C6 produced more from glycerol, and the amount of polymer accumulated was 19% higher. Recent studies (Claassens et al., 2020; Alagesan et al., 2018) highlight the importance of simultaneous CO_2 fixation while using glycerol, resulting in a mixotrophic lifestyle. Strittmatter et al. (2022) studied the role of a RuBisCO activase (CbbX) that participates in an efficient CBB cycle in *C. necator* H16 during glycerol degradation. The deletion of CbbX resulted in poor growth, highlighting the strong dependence on carbon fixation through the CBB cycle for glycerol utilization.

VFA are a byproduct of anaerobic digestion (AD), a process where organic matter is degraded and converted to methane in absence of oxygen. The main byproduct of AD is digestate, which is still rich in VFA that can be valorized. Jawed et al. (2022) studied mixotrophic growth and PHA accumulation in *C. necator* H16 under three conditions: VFA, VFA plus CO_2, and the inclusion of H_2 as an additional energy source. The results showed a higher PHA accumulation when cultures were grown mixotrophically with additional H_2. In another work, mixotrophic growth on glucose, acetate or glycerol as organic carbon source was compared, revealing that mixotrophic growth was faster than individual heterotrophic or chemolithotrophic growth (Amer and Kim, 2023). Interestingly, *C. necator* was found to switch from heterotrophic to chemolithotrophic/mixotrophic conditions in less than twelve hours. This metabolic adaptability highlights the potential for developing biotechnological processes focused on PHA production, utilizing mixotrophic growth to shorten the biomass accumulation phase thanks to the higher growth rate that can be achieved.

Sugars are among the most favorable and energy-efficient substrates for biomass accumulation, but the inability of *C. necator* to use glucose limits its applicability for PHA production from sources such as cellulose and starch. Given the rapid growth and high biomass yield that can be achieved with sugary feedstocks, it is worthwhile to expand the trophic capabilities of *C. necator* by mutagenesis and genetic engineering. Even adaptive evolution towards glucose uptake without mutagenic treatment was described, incubating the microorganism with high levels of glucose for a time period of around 70 h (Franz et al., 2012), achieving both growth and PHA accumulation of 45% *w*/w of the cell dry weight (CDW). The mutant strain DSM 545 has been used in several studies due to its ability to take up glucose, which allows utilization of sucrose-, cellulose- and starch-rich waste streams. In these studies, the first step usually consists in growing the microorganisms on glucose to accumulate biomass, and in the second step PHA accumulation is enhanced using another inexpensive carbon source, which is thus valorized. Cheese whey is a waste material available in large amounts, with a high concentration of lactose, and which causes disposal problems in the EU (Strøm-Andersen et al., 2019). To allow for lactose utilization, Povolo et al. (2010) used *C. necator* strain DSM 545 for testing PHA production from cheese whey by constructing a recombinant strain inserting the *Escherichia coli* lac operon in the chromosome of *C. necator*. The growth and PHA accumulation was compared using lactose, enzymatically hydrolysed whey permeate and non-hydrolysed whey permeate. While the wild-type strain did not grow on these media, the recombinant strain was able to grow and synthesize polymer from whey permeate and lactose. However, higher PHA accumulation after 48 h was observed when feeding hydrolysed whey permeate (30% CDW) with respect to the non-hydrolyzed counterpart (22% CDW).

Agricultural waste and crop residues such as dairy waste, date seeds, grain crops or starch contain a large amount of starchy biomass, which may provide valuable feedstock for the production of PHA but cannot be utilized as such by *C. necator*. Commercial amylase cocktails can be used to hydrolyze starch to monosaccharides, like glucose, which *C. necator* DSM 545 can use. However, this is a costly process, so alternative strategies were researched. A recent work described the development of a recombinant amylolytic strain of *C. necator* DSM 545 for PHA production from starchy residues (Brojanigo et al., 2022). A high biomass yield was observed, and PHA production was as high as 5.92, 5.78 and 3.65 g/L from raw corn starch, broken rice and purple sweet potato waste, respectively. Yousuf and Winterburn (2016) demonstrated that *C. necator* H16 can grow with yields between 0.26 and 0.46 g/g and accumulate around 73–75% CDW of PHA from date seeds, which

represent an important waste stream due to their high nutrient content. Genetic engineering approaches can have a positive impact on the PHA yield from date byproducts, as well as the composition of the polymer. In a work investigating the bioconversion of date seed oil, a recombinant strain of *C. necator* H16 was engineered by replacing genes encoding PHA synthase and pyrroline-5-carboxylate reductase with more efficient homologs from other microorganisms (Budde et al., 2011). Purama et al. (2018) also used this engineered strain to convert date-derived products as carbon source for *C. necator*, namely date seed oil and date molasses. The maximum CDW obtained using the optimum oil concentration (10 g/L) was 7.6 g/L with a PHA content of 81% of CDW with concomitant 6.2 g/L total PHA. When using date molasses (20 g/L), CDW (4.2 g/L) and PHA content (32% CDW) were lower than the values observed using date oil. Chicory roots are a byproduct of hydroponic salad cultivation which contain a high percentage of fructose and glucose in dry weight. Hence, their bioconversion to PHA was studied, comparing the productivity of strains H16, DSM 545, and DSM 531. As DSM 545 was the only strain able to utilize glucose, its productivity of 0.15 g/(L·h) and PHA content (78%) were strikingly superior to the other strains. However, sugar availability in the substrate was dependent on pretreatment with inulinase (Haas et al., 2015).

Molasses are by-products that are mainly found in sugarcane or sugar beet industry. They are characterized by a high amount of sucrose, but also contain vitamins and a spectrum of mineral elements which are useful to support the growth of the strains used for PHA production. However, molasses need to be pretreated to convert sucrose into its monomers, which are readily utilized by *C. necator*. Ertan et al. (2021) studied enzymatic and chemical methods to perform sugar hydrolysis and reported that acid treatment resulted in higher PHA production, while enzymatic treatment resulted in higher cell weights for *C. necator* ATCC 25207. The maximum PHA production was observed with sulphuric acid pretreatment: 2.36 g/L PHA were obtained when working in shake flasks and 15.28 g/L when working in a bioreactor, with a PHA content of 53% CDW. These values are higher than those obtained by other authors using acid pretreatment, such as Sen et al. (2019), who reported a PHA production of 0.78 g/L (27.3% PHA content) using cane molasses, or Baei et al. (2011) who obtained 1.30 g/L of PHA when using a mix of cane and sugar beet molasses. The use of enzymatic (invertase or baker's yeast) or acid (HCl or H_2SO_4) hydrolyzed molasses for evaluating *C. necator* DSM 545 growth was studied (Dalsasso et al., 2019) revealing that invertase treatment was the most effective for biomass formation, with a PHA accumulation of 11.70 g/L representing 56% of the CDW. While these are promising results, applicability of an enzymatic treatment in large scale may present cost-effectiveness issues. Kiselev et al. (2022) studied growth and PHA production of *C. necator* B-10646 from sugar beet molasses using enzymatic pretreatment for hydrolysing. It was determined that reducing excess sugar and nitrogen was necessary to facilitate growth. However, diluting the substrate resulted in a phosphorus deficiency. To address this issue, a method for controlling feeding was developed, involving the addition of extra glucose and phosphorus to ensure biomass growth (approximately 80–85 g/L), achieving a final polymer content up to 80% of CDW. An alternative to pretreatments is to engineer *C. necator*, enabling it to consume raw molasses. For instance, Jo et al. (2021) developed a recombinant strain which can hydrolyse sucrose into glucose and fructose. When crude sugarcane molasses were added to the culture, growth was inhibited, probably due to the presence of some compounds as light or heavy metal ions (Liu et al., 2008); the negative effect continued even when the substrate was diluted. The substrate was pretreated with active charcoal since it has low cost and does not affect the total sugar quantity. After treatment, a high PHA content of 82.5% of CDW with a high biomass production (20.3 g/L CDM) was observed.

As it has been described, many substrates can be used as carbon source for PHA production, with varying efficiencies. Zhila et al. (2021) compared different substrates, studying the properties of PHAs produced by the strain *C. necator* IPB/SFU-1 when using different organic carbon sources: sugars (fructose and glucose), purified glycerol, different plant oils, and fatty acids. Among the waste products tested in the study, palm oil was notable for the high percentage of accumulated PHA (80%) and a PHA/substrate yield of almost 50% (Table 2). The chemical composition and properties of PHA were influenced by the type of the carbon source used. For instance, fatty acids or plant oils produce PHAs with a variety of monomers, including 3HV or other co-monomers whereas sugars such as fructose and glucose have been found to produce PHAs containing mainly 3HB monomers. The monomer composition can significantly impact the material properties of PHAs (Section 3.2) and plays a crucial role in their biodegradability and biocompatibility (Cai et al., 2023; Miu et al., 2022). Another aspect to consider is the suitability of the strain to the consumption of the substrate of choice. For example, strains which can readily metabolize glucose, such as DSM 545 or IPB/SFU-1, are well-suited for the bioconversion of sugar-rich substrates. However, adaptive evolution has been demonstrated more than once to improve the tolerance and viability of substrates in *C. necator* (González-Villanueva et al., 2019; Franz et al., 2012). These aspects highlight the significance of selecting an appropriate carbon source and bacterial strain for PHA production depending on the final industrial application.

4.2. Inorganic waste streams

Apart from all the renewable and inexpensive carbon sources that *C. necator* can consume heterotrophically, there is an important carbon source that the microorganism is able to consume in chemolithotrophy and convert into PHA: carbon dioxide. CO_2 is the major greenhouse gas produced nowadays and its emission from the combustion of fossil fuels implies a severe environmental problem, which leads to an urgent need of not only reducing the production sources but also removing the gas produced. One alternative that has gained great attention in the last years is using the gas as a raw material to produce valuable chemicals as PHA, sucrose, lipochitooligosaccharides, etc. *C. necator* can assimilate CO_2 through the CBB cycle, as described in Section 3.1. However, bioconversion of CO_2 to PHA is a very energy-consuming and potentially slow process, as CO_2 needs to be fixed into the building blocks for PHA monomers before it can be accumulated. Furthermore, the process of chemolithotrophic growth is heavily dependent on the accessibility of the microorganism to the necessary gasses (i.e., CO_2, O_2, H_2), which usually translates into the need for an efficient system for gas-liquid mass transfer. Thus, many systems and reactor configurations have been proposed to optimize this process (Table 2). The first works describing CO_2 conversion into PHA by *C. necator* reported a biomass accumulation of 60 g/L and 60% PHA content using a gas mixture of H_2:CO_2:O_2 = 75:10:15 (Ishizaki and Tanaka, 1991). Some years later, Tanaka et al. (1995) reported a higher biomass concentration of 91 g/L and 67% PHA accumulation working with a continuous stirred tank bioreactor in which a specific recirculation system for enhancing gas transfer was implemented. Air-lift configuration was also evaluated as an option to increase the volumetric mass transfer coefficient (k_La) and enhance PHA production. The authors reported a maximum biomass accumulation of 60 g/L and PHA content of 82%, again using a gas mixture of H_2:CO_2:O_2 = 75:10:15 (Taga et al., 1997). The maximum PHA content was achieved working under oxygen limitation. The same authors also studied the addition of a surface-active reagent (carboxymethylcellulose, CMC) to affect the rheology of the liquid culture. The addition of CMC resulted in an enhancement of PHA production rate while oxygen concentration was maintained at a very low level. Recently, growth and PHA accumulation of *C. necator* H16 were studied in a bioreactor equipped with continuous gas feeding (Lambauer and Kratzer, 2022). The authors tried different H_2:CO_2:O_2 proportions, achieving a maximum biomass composition of 13 g/L CDW with a PHA content of 10.2 g/L (78%) when the dissolved oxygen was kept below 1.1 mg/L. A follow-up study by these researchers optimized the bioreactor set-up to automate and fine-tune the oxygen supply and to measure

the dissolved oxygen with high precision, finding that the optimal conditions for PHB production were achieved using 0.8 mg/L dissolved oxygen (Lambauer et al., 2023). PHA accumulation is usually triggered by stress conditions (Section 3.3). Regarding PHA accumulation from CO_2, a kinetic model was developed by Mozumder et al. (2015), based on experimental data, to determine the optimal gas proportions and nutrient limitations for PHA production. For chemolithotrophic growth in continuous systems, the authors observed that limitation of oxygen enhanced PHA production more than nitrogen limitation, with an optimal O_2:H_2 ratio of 2:7.

In the studies described above, a two-stage strategy was used for growing *C. necator*, where the first stage consisted in accumulating biomass with an organic carbon source such as fructose, and the second stage was performed to elicit the stress for PHA accumulation from CO_2. However, as in the studies with heterotrophic growth, recombinant strains have been created in the last years with the aim of developing single-step processes, avoiding the heterotrophic growth stage. Moreover, researchers have adopted metabolic engineering techniques to produce PHA from CO_2 more efficiently. For instance, a recombinant strain of *C. necator* was engineered with the aim of achieving PHA production simultaneous to growth. The strategy involved heterologous expression of a hemoglobin gene to improve oxygen utilization, as well as knockout of genes related to the central carbon metabolism, to redirect carbon fluxes to PHA synthesis, yielding 0.55 g/L cells and 50.4% PHA content (Tang et al., 2020). As CO_2 bioconversion yields strictly PHB, genetic engineering is necessary to obtain PHAs with more convenient monomer compositions. In a recent work, recombinant strains of *C. necator* H16 able to synthesize a copolymer of 3HB and 3-hydroxyhexanoate (3HHx) from fructose were investigated to test if the same monomer composition was obtained growing on H_2:CO_2:O_2 = 8:1:1. High PHA cellular contents were obtained, and bioconversion to the P(3HB-co-3HHx) copolymer was successful, with a maximum accumulation of around 86% (Tanaka et al., 2021). The control of monomer composition was proven feasible by constructing recombinant strains that harbored thioesterases and PHA synthases with different chain length preferences (Section 3.2, Nangle et al., 2020).

Besides using H_2:CO_2:O_2 mixtures for chemolithotrophic growth, synthetic gas (syngas), which is one of the most inexpensive and flexible substrates derived from biomass gasification, can also be used as a carbon source for PHA synthesis. In addition to CO_2, syngas contains a significant proportion of CO, which is not consumed by wild-type *C. necator* and can be toxic for growth. A PHA accumulation of 70–75% CDW was observed in the presence of 5–25% CO under chemolithotrophic conditions (Volova et al., 2002). However, adding CO to a culture growing on a H_2:CO_2:O_2 gas mixture resulted in a tolerance of only up to 10% CO (Yu et al., 2013). In general, *C. necator* H16 growth decreases with increasing concentrations of CO, and most results indicate 10% CO as the maximum tolerated partial pressure. Similar or lower concentrations are frequently reported for syngas, but in the case of higher CO content, other strategies can be applied. One work described the use of nanoscaled cellulose particles with an enzyme complex mobilized on *C. necator* that allowed the conversion of CO into CO_2, to allow its utilization by the bacterium (Shin et al., 2021). In that way, a biomass accumulation of 33.8 g/L with 42% PHA was observed with syngas composition of H_2:CO_2:O_2:CO = 20:20:20:40. Another possibility is to construct recombinant strains expressing an oxygen-tolerant carbon monoxide dehydrogenase (CODH) to allow the conversion of CO into CO_2 and the subsequent use as carbon source. This approach was demonstrated in *C. necator* H16, showing an increase in PHA synthesis by >20% using a gas mixture of H_2:CO_2:N_2:CO = 40:10:10:40 (Heinrich et al., 2018). The authors of this study also note that, while growth on CO as a carbon source is not possible without genetic engineering, in the case of *C. necator* it is advantageous to explore this aspect, as its hydrogenases and cytochromes have a high tolerance to CO, contrary to many other aerobic organisms.

5. *C. necator* metabolic models and predictions

In GSMMs, reactions and metabolites collectively define a metabolic network and the rate (flux) of each reaction determines the production or consumption rate of the corresponding metabolites. Therefore, these models effectively capture the metabolic capabilities of an organism. The most common mathematical method to study GSMMs and leverage the information that they contain is FBA. This analysis generates a system of linear equations from the metabolic reactions and their constraints, which are dictated by stoichiometry. Then, an objective function is defined, and the optimal flux distribution is identified by linear programming. Usually, the objective function is maximization of biomass, yielding as a result of FBA the growth rate according to the given constraints; however, other reactions can be maximized or minimized. Changes in nutrient availability, as well as variations in the rate of a reaction, e.g., due to genetic variants, or condition-specific gene expressions, can be simulated in the model by changing reaction constraints. Repeating FBA allows then comparing growth rates in different scenarios, allowing for in silico hypothesis testing (Orth et al., 2010).

Efforts for metabolic modeling of *C. necator* have been focused almost entirely on strain H16. Two GSMMs have been published for this strain: RehMBEL1391 and iCN1361 (Pearcy et al., 2022; Jahn et al., 2021; Park et al., 2011). The first model was published in 2011, using as a starting point the reactions annotated in the Kyoto Encyclopedia of Genes and Genomes (KEGG) database for the organism, which in turn were based on the genome sequence published in 2006 (Park et al., 2011; Pohlmann et al., 2006). KEGG reactions were then integrated with data from other databases and literature. Despite being based on KEGG reactions, unique reaction and metabolite IDs from the database were not used in the model files. Furthermore, the files made available in the paper are in PDF format, which is not computer readable. As a result, the original model is difficult to automatically parse and update, and it is especially problematic to map the model's metabolites to stable IDs in databases due to the ambiguity that can arise from naive string comparison methods (Pham et al., 2019). Successive efforts to improve model readability involved conversion of the model to the standard SBML format (Peyraud et al., 2016) and addition of annotations and ID mapping for genes, reactions, and metabolites (Jahn et al., 2021). Importantly, the latest version of RehMBEL1391 is validated with resource balance analysis, a variant of FBA, and simulation results are compared with protein quantification data. The most recent model, iCN1361, is described in Pearcy et al., 2022. This model was developed from BioCyc to ensure a stable namespace with unambiguous compound and reaction identifiers. Also in this case, model validation involved the comparison of FBA results with experimental data. The predictive power of the model was assessed with respect to carbon source viability, central carbon metabolic fluxes, gene essentiality, and gene expression in optimal growth conditions and nitrogen-limited medium (Pearcy et al., 2022) (Table 3).

Despite the availability of highly comprehensive genome-scale models, most metabolic modeling applications employ reduced networks, usually composed of central carbon metabolic pathways and a

Table 3
Summary statistics of published genome-scale metabolic models for *C. necator* H16.

GSMM name	Namespace	Reactions	Metabolites	Reference
RehMBEL1391	Reactions: EC numbers, gene locus tags Metabolites: non-systematic	1391	1171	Park et al., 2011
RehMBEL1391 - updated	BiGG	1538	1172	Jahn et al., 2021
iCN1361	EcoCyc	1292	1263	Pearcy et al., 2022

few other metabolic routes to account for uptake and synthesis of specific compounds, according to the applications or the biological aspects under investigation. Works based on reduced networks often rely on elementary mode (EM) analysis and yield space analysis (Song and Ramkrishna, 2009; Schuster et al., 2000). EM analysis is essentially an enumeration of minimal sub-networks that operate at the steady state conditions. Due to the combinatorial nature of this method, working with small networks is necessary (Lopar et al., 2013; Schuster et al., 2000). Based on the substrates and products under observation, a yield space can be defined, which usually involves the biomass/substrate yield and the product/substrate yield as axes. EMs are then analyzed to filter out inactive ones and assess the coordinates of active EMs in the yield space. Real data from cultivations can be mapped to the yield space as well, and the comparison with simulated data allows to establish connections between biomass/products formation and the metabolic state of the cells. This framework was applied in several works to investigate metabolic states respectively related to glucose to PHA, glycerol to PHA, and carbon dioxide to biofuels conversions (Unrean et al., 2019; Lopar et al., 2014; Lopar et al., 2013) (Table 4).

Another popular approach to study *C. necator* industrial applications in reduced metabolic networks is represented by hybrid cybernetic models (HCM) (Song et al., 2009; Kim et al., 2008). This framework, like yield analysis, is implemented on top of EM analysis. HCMs are useful for the study of cultivation dynamics and consider two main aspects in addition to metabolic flux rates: the mass balance of biomass and external metabolites, which is described by state equations; and the regulation of enzymes, which is described by cybernetic variables. This approach has the important advantage of enabling the simulation of dynamics in processes characterized by multiple phases, without reparametrization of the model to reflect the distinct metabolic states undergone by the cells. One of the earliest examples of HCMs to study *C. necator*-mediated bioprocesses is the work by Franz et al. (2011), which modeled the dynamics of PHA consumption and production in a continuous bioreactor. Other relevant applications of the HCM

Table 4
Metabolic modeling approaches developed around potential *C. necator* industrial applications.

Model	Approaches	Strain	Application	Advantages of model	Reference
Metabolic network of central carbon metabolism and PHA formation on lactate; state equations to describe substrate and product kinetics	Least-squares mass balance analysis	H16	Investigation of production of PHA from sugars via lactate employing a mixed culture of *C. necator* and L. *delbrueckii*	Well describes mixed culture dynamics in a batch reactor	Katoh et al., 1999
Metabolic network of heterotrophic central carbon metabolism and PHA formation; cybernetic variables to describe enzyme activity; state equations to describe substrate and product kinetics	Elementary mode analysis Yield space analysis Hybrid cybernetic modeling	H16	Investigation of PHA production from fructose in batch and continuous bioreactors	Well describes PHA dynamics in batch and continuous reactors; accounts for PHA consumption allowing for more accuracy	Franz et al., 2011
Metabolic network of heterotrophic central carbon metabolism and PHA formation; state equations to describe substrate and product kinetics	Elementary mode analysis Yield space analysis	DSM 545	Five-stage continuous cultivation for PHA production from glucose	Well describes PHA synthesis and microbial growth dynamics in continuous multistage reactor	Lopar et al., 2013
Metabolic network of heterotrophic central carbon metabolism, glycerol uptake, and PHA formation	Elementary mode analysis Yield space analysis	DSM 545	Two-stage cultivation for PHA production from glycerol	Identifies metabolic regimes that best explain observed biomass and PHA yields from glycerol; suggests metabolic engineering targets to improve PHB production from glycerol	Lopar et al., 2014
Metabolic network of central carbon heterotrophic metabolism and isopropanol formation; cybernetic variables to describe enzyme activity; state equations to describe substrate and product kinetics	Elementary mode analysis Yield space analysis Hybrid cybernetic modeling	Re2133/pEG7c (Grousseau et al., 2014)	Presentation of the hybrid cybernetic model approach using a batch culture for conversion of fructose to isopropanol with an engineered *C. necator* strain	Well describes isopropanol synthesis by an engineered strain in a batch reactor	Ternon et al., 2014
Metabolic network of central carbon metabolism, glycerol uptake, and PHA formation	Steady state metabolic flux analysis	H16	Integration of carbon labeling data into the core metabolic network to study heterotrophic and mixotrophic growth on fructose and glycerol	Well describes changes in the core carbon metabolism in heterotrophy vs. mixotrophy; uncovers role of CBB cycle in heterotrophy	Alagesan et al., 2018
Metabolic network of chemolithotrophic core metabolism, hexadecanol formation, isobutanol formation	Flux balance analysis Elementary mode analysis Yield space analysis	H16	Chemolithotrophic production of biofuels and model-guided genetic engineering to improve yield	Identifies potential gene targets for deletion and overexpression to maximize biofuel production from CO_2	Unrean et al., 2019
Metabolic network including fructose and acetate uptake and PHA formation; cybernetic variables to describe enzyme activity; state equations to describe substrate and product kinetics	Elementary mode analysis Yield space analysis Hybrid cybernetic modeling	H16	Simulation of PHA accumulation by co-feeding fructose and acetate	Simulates the effects of different ratios between co-fed substrates on PHA productivity	Duvigneau et al., 2020
Metabolic network of central carbon metabolism, glycerol and nitrogen uptake and PHA formation	Dynamic flux balance analysis (DFBA) Thermodynamic-based flux estimation to constrain DFBA results	DSM 545	Study of glycerol conversion to PHA and evaluation of PHA accumulation strategies in four batch cultures in different conditions	Well describes the energy and redox state of the cell in PHA production; underlines the importance of uncoupling biomass growth and PHA accumulation for best productivity	Sun et al., 2020
Metabolic network of central carbon metabolism, uptake of formate and PHA formation	Elementary mode analysis Yield space analysis Max-min driving force analysis	H16	Study of formate conversion to PHA and model-guided genetic engineering to improve yield	Identifies heterologous reactions improving PHA productivity (experimentally verified measuring PHA accumulation increase from 52.3% to 77.9%)	Janasch et al., 2022

framework include the work of Ternon et al. (2014), who employed HCM to simulate the effects of a genetic engineering strategy for fructose conversion to biofuels, and the work of Duvigneau et al. (2020), who applied the framework to simulate the behavior of a co-culture of *C. necator* and *Lactobacillus delbrueckii* (Table 4). These works show the flexibility of the framework and suggest potential applications more targeted to circular economy, especially in devising processes where the input of bioconversion are waste streams.

Overall, GSMMs of *C. necator* are a valuable knowledge base, but the most frequent applications involve reduced networks. One possible reason for this is that PHA production is a relatively simple process and majorly interacts with central carbon metabolism. The same can be said for other frequently seeked bioproducts, such as biofuels. Therefore, most reactions involving secondary metabolites can be overlooked or lumped in the biomass reaction. However, since the main reason for network reduction is the algorithmic complexity of approaches such as EM and HCMs, it would be interesting to devise a strategy to simulate and validate fluxes at genome scale, possibly to uncover alternative metabolic states or explore more in depth the whole metabolism. On the other hand, as the knowledge of genome-scale metabolism is limited even for model organisms, GSMMs need to be constantly updated to reflect advances in research. Indeed, some pathways may be lumped into pseudo-reactions, while enzymes that can take classes of compounds as substrates may be encoded in a simplified way, e.g., the beta-oxidation pathway involving the pseudo-metabolite acyl-CoA. Some "known unknowns" regard details such as lipopolysaccharide synthesis, whose definition in the model depends on the information regarding lipopolysaccharide composition, which is not yet available for *C. necator* (Pearcy et al., 2022). While full characterization of *C. necator* metabolism will reasonably take years, GSMMs can help identify critical components to be investigated. Another element that is overlooked in the current *C. necator* literature is the definition of the biomass objective function. It is often remarked that the composition of biomass can vary dramatically under different environmental conditions (Zuñiga et al., 2016). It is reasonable to think that PHA accumulation heavily influences biomass composition, however this aspect is never touched upon in scientific literature on *C. necator* models. One important limitation experienced by the authors while dealing with existing GSMMs in relation to PHAs is the lack of modeling of monomers other than 3HB and their incorporation in the polymer. There is potential in the setup of a modeling strategy to account for different monomers and estimate their proportion according to feedstock composition. In general, the potential of GSMMs to guide culturing or genetic engineering approaches in *C. necator* seem to be underexplored.

From a practical standpoint, a gradual albeit still limited transition from descriptive to predictive models can be appreciated. In early studies, in silico modeling had the main purpose of explaining central metabolism activity underlying observed microbial growth and PHA production while verifying the agreement with experimental data. In these cases, the focus was therefore on testing model validity (Franz et al., 2011; Katoh et al., 1999). With the progressive improvement of the models, they were also used to identify critical pathways, flux bottlenecks (and subsequently, the best candidates for genetic modifications) and the response to perturbations (Lopar et al., 2014; Alagesan et al., 2018; Unrean et al., 2019; Sun et al., 2020). Only recently, the predictive value of metabolic models has begun to be explored more systematically, also thanks to the introduction of novel techniques (Unrean et al., 2019; Janasch et al., 2022). For example, they were used to identify the best process parameters and substrate ratios before process setup, with the aim of saving time and resources avoiding repeated trial-and-error experiments (Duvigneau et al., 2020; Sun et al., 2020). Notably, very few works attempt to quantify the impact of the adoption of metabolic models, for example by comparing product yields with and without process optimization (Janasch et al., 2022). Given the wide establishment of GSMMs and akin models in other areas of metabolic engineering and bioprocessing, there is thus ample potential and unexplored territory for their application in the future.

Interestingly, most investigations involving reduced networks are focused on heterotrophic growth, while only a couple of works deal with modeling of chemolithotrophic or mixotrophic processes (Table 4). Chemolithotrophic growth involving gaseous carbon and energy sources has an additional limitation in correctly estimating the gas-liquid transfer, which is highly dependent on process parameters such as temperature, pressure, reactor and agitation system employed. The kinetic model proposed by Mozumder and collaborators for chemolithotrophic PHA production is a first step towards the development of accurate modeling strategies for this application. The establishment of efficient bioconversion processes from CO_2 to PHA would be significantly aided by the possibility to simulate gas consumption kinetics in a variety of scenarios. Therefore, integration of these kinetics with metabolic models is desirable.

6. Conclusions

Currently, there is an ample body of scientific literature involving *C. necator* which touches on several aspects, such as its environmental and metabolic versatility, its potential as a platform chemical producer, and the details of its metabolism. However, some areas represent interesting starting points for further research. For example, information is still lacking on the intra-species variability of the microorganism. For many strains available in cell banks, the genome sequence is not publicly available. A few mutants have been characterized in order to identify the causative mutations of their phenotypes, but for many others, this characterization is still missing. Physiological differences and benchmarks between *C. necator* strains are also underexplored. A thorough understanding of intra-species variability could maximize the ability to leverage the potential of this microorganism for biotechnological applications. Another important subject is represented by the development of applications related to bioeconomy and circular economy. Indeed, many bioprocesses have been successfully set up which allow to repurpose waste streams using *C. necator*, with promising results. Notably, processes involving heterotrophic growth are the most frequent in the literature, while there is room for the development of chemolithotrophic processes, which could be relevant in the context of CO_2 capture. Finally, the use of metabolic models for improvement of biotechnological processes is well-established for *C. necator* and in many cases allows to identify metabolic bottlenecks or to accurately characterize the biological mechanisms that regulate process dynamics. In the authors' opinion, the use of GSMMs is surprisingly limited, in favor of reduced networks. Furthermore, possibly as a result of not being exploited often, currently available *C. necator* GSMMs do not account for aspects such as the variation of the biomass equation along with intracellular PHA percentage and the existence of distinct PHA precursors and their relation to polymer composition. Importantly, the ability to uptake VFA is not completely represented in the models, particularly RehMBEL1391. As PHA synthesis in the presence of VFA results in variations in the polymer composition, and as VFA are common compounds in carbon-rich waste streams, this represents a point worth expanding on. Consequently, as a future perspective, there is potential in the setup of a modeling strategy to account for different PHA precursors and estimate their proportion according to feedstock composition. In general, GSMMs can be exploited in combination with "-omic" data to develop novel culturing or genetic engineering approaches in *C. necator*.

CRediT authorship contribution statement

Maria Silvia Morlino: Conceptualization, Formal analysis, Writing – original draft, Visualization. **Rebecca Serna García:** Writing – original draft, Writing – review & editing, Visualization. **Filippo Savio:** Writing – review & editing, Visualization. **Guido Zampieri:** Writing – review & editing, Supervision. **Tomas Morosinotto:** Project administration, Writing – review & editing, Funding acquisition. **Laura Treu:** Project

administration, Writing – review & editing, Supervision, Funding acquisition. **Stefano Campanaro:** Writing – review & editing, Supervision, Funding acquisition.

Declaration of Competing Interest

The authors declare that they have no known competing financial interests or personal relationships that could have appeared to influence the work reported in this paper.

Acknowledgements

Funding: this work was financially supported by the project "Harnessing potential of biological CO2 capture for Circular Economy" (CooCE) (Project No 327331) which is co-funded by the European Commission (receiving funding from European Union's Horizon 2020 Grant agreement No. 691712) and national funds (Ministero dell'Università e Ricerca MUR, Italy) under the ERA-Net Cofund ACCELERATING CCS TECHNOLOGIES (ACT). This study was carried out within the MICS (Made in Italy – Circular and Sustainable) Extended Partnership and received funding from the European Union Next-GenerationEU (PIANO NAZIONALE DI RIPRESA E RESILIENZA (PNRR) – MISSIONE 4 COMPONENTE 2, INVESTIMENTO 1.3 – D.D. 1551.11-10-2022, PE00000004). This manuscript reflects only the authors' views and opinions, neither the European Union nor the European Commission can be considered responsible for them.

References

Abbey, A.-M.I., Beaudette, L.A., Lee, H., Trevors, J.T., 2003. Polychlorinated biphenyl (PCB) degradation and persistence of a GFP-marked *Ralstonia eutropha* H850 in PCB-contaminated soil. Appl. Microbiol. Biotechnol. 63, 222–230. https://doi.org/10.1007/s00253-003-1380-x.

Ahrens, W., Schlegel, H.G., 1972. Carbon dioxide requiring mutants of *Hydrogenomonas eutropha* strain H 16. I. Growth and CO_2-fixation. Arch. Mikrobiol. 85, 142–152. https://doi.org/10.1007/BF00409296.

Alagesan, S., Minton, N.P., Malys, N., 2018. ^{13}C-assisted metabolic flux analysis to investigate heterotrophic and mixotrophic metabolism in *Cupriavidus necator* H16. Metabolomics Off. J. Metabolomic Soc. 14, 9. https://doi.org/10.1007/s11306-017-1302-z.

Altschul, S.F., Gish, W., Miller, W., Myers, E.W., Lipman, D.J., 1990. Basic local alignment search tool. J. Mol. Biol. 215, 403–410. https://doi.org/10.1016/S0022-2836(05)80360-2.

Amer, A., Kim, Y., 2023. Minimizing the lag phase of *Cupriavidus necator* growth under autotrophic, heterotrophic, and mixotrophic conditions. Appl. Environ. Microbiol. 89, e02007–e02022. https://doi.org/10.1128/aem.02007-22.

Amobonye, A., Bhagwat, P., Raveendran, S., Singh, S., Pillai, S., 2021. Environmental impacts of microplastics and nanoplastics: a current overview. Front. Microbiol. 12.

Asnicar, F., Thomas, A.M., Beghini, F., Mengoni, C., Manara, S., Manghi, P., Zhu, Q., Bolzan, M., Cumbo, F., May, U., Sanders, J.G., Zolfo, M., Kopylova, E., Pasolli, E., Knight, R., Mirarab, S., Huttenhower, C., Segata, N., 2020. Precise phylogenetic analysis of microbial isolates and genomes from metagenomes using PhyloPhlAn 3.0. Nat. Commun. 11, 2500. https://doi.org/10.1038/s41467-020-16366-7.

Baei, S.M., Najafpour, G.D., Younesi, H., Tabandeh, F., Issazadeh, H., Khodabandeh, M., 2011. Growth kinetic parameters and biosynthesis of polyhydroxybutyrate in *Cupriavidus necator* DSMZ 545 on selected substrates. Chem. Ind. Chem. Eng. Q. 17, 1–8.

Bar-Joseph, Z., Gifford, D.K., Jaakkola, T.S., 2001. Fast optimal leaf ordering for hierarchical clustering. Bioinformatics 17, S22–S29. https://doi.org/10.1093/bioinformatics/17.suppl_1.S22.

Bartha, R., 1962. Physiologische Untersuchungen über den chemolithotrophen Stoffwechsel neu isolierter *Hydrogenomonas*-Stämme. [Physiological investigations on the chemolithotrophic metabolism of newly isolated *Hydrogenomonas* strains.]. Arch. Für Mikrobiol. 41, 313–350. https://doi.org/10.1007/BF00403610.

Bowien, B., 1970. Hexose Degradation and Pentose Biosynthesis in *Hydrogenomonas* (Doctoral thesis). University of Goettingen.

Bowien, B., Schlegel, H.G., 1981. Physiology and biochemistry of aerobic hydrogen-oxidizing bacteria. Annu. Rev. Microbiol. 35, 405–452. https://doi.org/10.1146/annurev.mi.35.100181.002201.

Brojanigo, S., Gronchi, N., Cazzorla, T., Wong, T.S., Basaglia, M., Favaro, L., Casella, S., 2022. Engineering *Cupriavidus necator* DSM 545 for the one-step conversion of starchy waste into polyhydroxyalkanoates. Bioresour. Technol. 347, 126383. https://doi.org/10.1016/j.biortech.2021.126383.

Budde, C.F., Riedel, S.L., Willis, L.B., Rha, C., Sinskey, A.J., 2011. Production of poly(3-hydroxybutyrate-co-3-hydroxyhexanoate) from plant oil by engineered *Ralstonia eutropha* strains. Appl. Environ. Microbiol. 77, 2847–2854. https://doi.org/10.1128/AEM.02429-10.

Byrom, D., 1987. Polymer synthesis by microorganisms: technology and economics. Trends Biotechnol. 5, 246–250. https://doi.org/10.1016/0167-7799(87)90100-4.

Cai, F., Lin, M., Jin, W., Chen, C., Liu, G., 2023. Biosynthesis of poly(3-hydroxybutyrate-co-3-hydroxvalerate) from volatile fatty acids by *Cupriavidus necator*. J. Basic Microbiol. 63, 128–139. https://doi.org/10.1002/jobm.202200448.

Castro-Sowinski, S., Burdman, S., Matan, O., Okon, Y., 2010. Natural functions of bacterial Polyhydroxyalkanoates. In: Chen, G.G.-Q. (Ed.), Plastics from Bacteria: Natural Functions and Applications, Microbiology Monographs. Springer, Berlin, Heidelberg, pp. 39–61. https://doi.org/10.1007/978-3-642-03287-5_3.

Cavalheiro, J.M.B.T., de Almeida, M.C.M.D., Grandfils, C., da Fonseca, M.M.R., 2009. Poly(3-hydroxybutyrate) production by *Cupriavidus necator* using waste glycerol. Process Biochem. 44, 509–515. https://doi.org/10.1016/j.procbio.2009.01.008.

Chen, G.-Q., 2010. Plastics completely synthesized by bacteria: Polyhydroxyalkanoates. In: Chen, G.G.-Q. (Ed.), Plastics from Bacteria: Natural Functions and Applications, Microbiology Monographs. Springer, Berlin, Heidelberg, pp. 17–37. https://doi.org/10.1007/978-3-642-03287-5_2.

Claassens, N.J., Scarinci, G., Fischer, A., Flamholz, A.I., Newell, W., Frielingsdorf, S., Lenz, O., Bar-Even, A., 2020. Phosphoglycolate salvage in a chemolithoautotroph using the Calvin cycle. Proc. Natl. Acad. Sci. 117, 22452–22461. https://doi.org/10.1073/pnas.2012288117.

Cramm, R., 2009. Genomic view of energy metabolism in *Ralstonia eutropha* H16. Microb. Physiol. 16, 38–52. https://doi.org/10.1159/000142893.

Cramm, R., Pohlmann, A., Friedrich, B., 1999. Purification and characterization of the single-component nitric oxide reductase from *Ralstonia eutropha* H16. FEBS Lett. 460, 6–10. https://doi.org/10.1016/S0014-5793(99)01315-0.

Dalsasso, R.R., Pavan, F.A., Bordignon, S.E., de Aragão, G.M.F., Poletto, P., 2019. Polyhydroxybutyrate (PHB) production by *Cupriavidus necator* from sugarcane vinasse and molasses as mixed substrate. Process Biochem. 85, 12–18. https://doi.org/10.1016/j.procbio.2019.07.007.

Dalton, B., Bhagabati, P., De Micco, J., Padamati, R.B., O'Connor, K., 2022. A review on biological synthesis of the biodegradable polymers polyhydroxyalkanoates and the development of multiple applications. Catalysts 12, 319. https://doi.org/10.3390/catal12030319.

Davis, D.H., Doudoroff, M., Stanier, R.Y., Mandel, M., 1969. Proposal to reject the genus *Hydrogenomonas*: taxonomic implications. Int. J. Syst. Evol. Microbiol. 19, 375–390. https://doi.org/10.1099/00207713-19-4-375.

de Koning, G., 1995. Physical properties of bacterial poly((R)-3-hydroxyalkanoates). Can. J. Microbiol. 41, 303–309. https://doi.org/10.1139/m95-201.

De Meyer, S.E., Fabiano, E., Tian, R., Van Berkum, P., Seshadri, R., Reddy, T., Markowitz, V., Ivanova, N.N., Pati, A., Woyke, T., Howieson, J., Kyrpides, N.C., Reeve, W., 2015. High-quality permanent draft genome sequence of the *Parapiptadenia rigida*-nodulating *Cupriavidus* sp. strain UYPR2.512. Stand. Genomic Sci. 10, 13. https://doi.org/10.1186/1944-3277-10-13.

Doi, Y., Segawa, A., Kawaguchi, Y., Kunioka, M., 1990. Cyclic nature of poly(3-hydroxyalkanoate) metabolism in *Alcaligenes eutrophus*. FEMS Microbiol. Lett. 67, 165–169. https://doi.org/10.1111/j.1574-6968.1990.tb13856.x.

Duvigneau, S., Dürr, R., Carius, L., Kienle, A., 2020. Hybrid cybernetic modeling of polyhydroxyalkanoate production in *Cupriavidus necator* using fructose and acetate as substrates. In: IFAC-Pap., 21st IFAC World Congress, 53, pp. 16872–16877. https://doi.org/10.1016/j.ifacol.2020.12.1211.

Edgar, R.C., 2018. Updating the 97% identity threshold for 16S ribosomal RNA OTUs. Bioinformatics 34, 2371–2375. https://doi.org/10.1093/bioinformatics/bty113.

Ertan, F., Keskinler, B., Tanriseven, A., 2021. Exploration of *Cupriavidus necator* ATCC 25207 for the production of poly(3-hydroxybutyrate) using acid treated beet molasses. J. Polym. Environ. 29, 2111–2125. https://doi.org/10.1007/s10924-020-02020-2.

Fetzer, I., Johst, K., Schäwe, R., Banitz, T., Harms, H., Chatzinotas, A., 2015. The extent of functional redundancy changes as species' roles shift in different environments. Proc. Natl. Acad. Sci. 112, 14888–14893. https://doi.org/10.1073/pnas.1505587112.

Franz, A., Song, H.-S., Ramkrishna, D., Kienle, A., 2011. Experimental and theoretical analysis of poly(β-hydroxybutyrate) formation and consumption in *Ralstonia eutropha*. Biochem. Eng. J. 55, 49–58. https://doi.org/10.1016/j.bej.2011.03.006.

Franz, A., Rehner, R., Kienle, A., Grammel, H., 2012. Rapid selection of glucose-utilizing variants of the polyhydroxyalkanoate producer *Ralstonia eutropha* H16 by incubation with high substrate levels. Lett. Appl. Microbiol. 54, 45–51. https://doi.org/10.1111/j.1472-765X.2011.03171.x.

Fricke, W.F., Kusian, B., Bowien, B., 2009. The genome organization of *Ralstonia eutropha* strain H16 and related species of the Burkholderiaceae. Microb. Physiol. 16, 124–135. https://doi.org/10.1159/000142899.

Gai, C.S., Lu, J., Brigham, C.J., Bernardi, A.C., Sinskey, A.J., 2014. Insights into bacterial CO_2 metabolism revealed by the characterization of four carbonic anhydrases in *Ralstonia eutropha* H16. AMB Express 4, 2. https://doi.org/10.1186/2191-0855-4-2.

Geissdoerfer, M., Savaget, P., Bocken, N.M.P., Hultink, E.J., 2017. The circular economy – a new sustainability paradigm? J. Clean. Prod. 143, 757–768. https://doi.org/10.1016/j.jclepro.2016.12.048.

González-Villanueva, M., Galaiya, H., Staniland, P., Staniland, J., Savill, I., Wong, T.S., Tee, K.L., 2019. Adaptive laboratory evolution of *Cupriavidus necator* H16 for carbon co-utilization with glycerol. Int. J. Mol. Sci. 20, 5737. https://doi.org/10.3390/ijms20225737.

Goris, J., Konstantinidis, K.T., Klappenbach, J.A., Coenye, T., Vandamme, P., Tiedje, J. M., 2007. DNA–DNA hybridization values and their relationship to whole-genome sequence similarities. Int. J. Syst. Evol. Microbiol. 57, 81–91. https://doi.org/10.1099/ijs.0.64483-0.

Grousseau, E., Lu, J., Gorret, N., Guillouet, S.E., Sinskey, A.J., 2014. Isopropanol production with engineered *Cupriavidus necator* as bioproduction platform. Appl.

Microbiol. Biotechnol. 98, 4277–4290. https://doi.org/10.1007/s00253-014-5591-0.
Gunsalus, I.C., Pederson, T.C., Sligar, S.G., 1975. Oxygenase-catalyzed biological hydroxylations. Annu. Rev. Biochem. 44, 377–407. https://doi.org/10.1146/annurev.bi.44.070175.002113.
Haas, C., Steinwandter, V., Diaz De Apodaca, E., Maestro Madurga, B., Smerilli, M., Dietrich, T., Neureiter, M., 2015. Production of PHB from chicory roots – comparison of three *Cupriavidus necator* strains. Chem. Biochem. Eng. Q. 29, 99–112. https://doi.org/10.15255/CABEQ.2014.2250.
Heinrich, D., Raberg, M., Steinbüchel, A., 2018. Studies on the aerobic utilization of synthesis gas (syngas) by wild type and recombinant strains of *Ralstonia eutropha* H16. Microb. Biotechnol. 11, 647–656. https://doi.org/10.1111/1751-7915.12873.
International Code of Nomenclature of Prokaryotes, 2019. Int. J. Syst. Evol. Microbiol. 69, S1–S111. https://doi.org/10.1099/ijsem.0.000778.
Ishizaki, A., Tanaka, K., 1990. Batch culture of *Alcaligenes eutrophus* ATCC 17697T using recycled gas closed circuit culture system. J. Ferment. Bioeng. 69, 170–174. https://doi.org/10.1016/0922-338X(90)90041-T.
Ishizaki, A., Tanaka, K., 1991. Production of poly-β-hydroxybutyric acid from carbon dioxide by *Alcaligenes eutrophus* ATCC 17697T. J. Ferment. Bioeng. 71, 254–257. https://doi.org/10.1016/0922-338X(91)90277-N.
Jahn, M., Crang, N., Janasch, M., Hober, A., Forsström, B., Kimler, K., Mattausch, A., Chen, Q., Asplund-Samuelsson, J., Hudson, E.P., 2021. Protein allocation and utilization in the versatile chemolithoautotroph *Cupriavidus necator*. eLife 10, e69019. https://doi.org/10.7554/eLife.69019.
Jain, C., Rodriguez-R, L.M., Phillippy, A.M., Konstantinidis, K.T., Aluru, S., 2018. High throughput ANI analysis of 90K prokaryotic genomes reveals clear species boundaries. Nat. Commun. 9, 5114. https://doi.org/10.1038/s41467-018-07641-9.
Janasch, M., Crang, N., Asplund-Samuelsson, J., Sporre, E., Bruch, M., Gynnå, A., Jahn, M., Hudson, E.P., 2022. Thermodynamic limitations of PHB production from formate and fructose in *Cupriavidus necator*. Metab. Eng. 73, 256–269. https://doi.org/10.1016/j.ymben.2022.08.005.
Jawed, K., Irorere, V.U., Bommareddy, R.R., Minton, N.P., Kovács, K., 2022. Establishing mixotrophic growth of *Cupriavidus necator* H16 on CO_2 and volatile fatty acids. Fermentation 8, 125. https://doi.org/10.3390/fermentation8030125.
Jenni, B., Realini, L., Aragno, M., Tamer, A.Ü., 1988. Taxonomy of non H_2-lithotrophic, oxalate-oxidizing bacteria related to *Alcaligenes eutrophus*. Syst. Appl. Microbiol. 10, 126–133. https://doi.org/10.1016/S0723-2020(88)80026-2.
Jo, S.Y., Sohn, Y.J., Park, S.Y., Son, J., Yoo, J.I., Baritugo, K.-A., David, Y., Kang, K.H., Kim, H., Choi, J., Rhie, M.N., Kim, H.T., Joo, J.C., Park, S.J., 2021. Biosynthesis of polyhydroxyalkanoates from sugarcane molasses by recombinant *Ralstonia eutropha* strains. Korean J. Chem. Eng. 38, 1452–1459. https://doi.org/10.1007/s11814-021-0783-7.
Johnson, B.F., Stanier, R.Y., 1971. Dissimilation of aromatic compounds by *Alcaligenes eutrophus*. J. Bacteriol. 107, 468–475.
Katoh, T., Yuguchi, D., Yoshii, H., Shi, H., Shimizu, K., 1999. Dynamics and modeling on fermentative production of poly (β-hydroxybutyric acid) from sugars via lactate by a mixed culture of *Lactobacillus delbrueckii* and *Alcaligenes eutrophus*. J. Biotechnol. 67, 113–134. https://doi.org/10.1016/S0168-1656(98)00177-1.
Kessler, B., Witholt, B., 1998. Synthesis, recovery and possible application of medium-chain-length polyhydroxyalkanoates: a short overview. Macromol. Symp. 130, 245–260. https://doi.org/10.1002/masy.19981300122.
Kim, J.I., Varner, J.D., Ramkrishna, D., 2008. A hybrid model of anaerobic *E. coli* GJT001: combination of elementary flux modes and cybernetic variables. Biotechnol. Prog. 24, 993–1006. https://doi.org/10.1002/btpr.73.
Kiselev, E.G., Demidenko, A.V., Zhila, N.O., Shishatskaya, E.I., Volova, T.G., 2022. Sugar beet molasses as a potential C-substrate for PHA production by *Cupriavidus necator*. Bioengineering 9, 154. https://doi.org/10.3390/bioengineering9040154.
Kohlmann, Y., Pohlmann, A., Schwartz, E., Zühlke, D., Otto, A., Albrecht, D., Grimmler, C., Ehrenreich, A., Voigt, B., Becher, D., Hecker, M., Friedrich, B., Cramm, R., 2014. Coping with anoxia: a comprehensive proteomic and transcriptomic survey of denitrification. J. Proteome Res. 13, 4325–4338. https://doi.org/10.1021/pr500491r.
Koller, M., 2019. Chemical and biochemical engineering approaches in manufacturing polyhydroxyalkanoate (PHA) biopolyesters of tailored structure with focus on the diversity of building blocks. Chem. Biochem. Eng. Q. 32, 413–438. https://doi.org/10.15255/CABEQ.2018.1385.
Koller, M., Braunegg, G., 2015. Biomediated production of structurally diverse poly (hydroxyalkanoates) from surplus streams of the animal processing industry. Polimery 60, 298–308. https://doi.org/10.14314/polimery.2015.298.
Koller, M., Salerno, A., Braunegg, G., 2013. Polyhydroxyalkanoates: Basics, production and applications of microbial biopolyesters. In: Bio-Based Plastics. John Wiley & Sons, Ltd, pp. 137–170. https://doi.org/10.1002/9781118676646.ch7.
König, C., 1967. Über die Kultur von *Hydrogenomonas* H16 im Chemostaten unter chemoorganotrophen Bedingungen. [On the cultivation of *Hydrogenomonas* H16 in chemostat under chemoorganotrophic conditions.]. Ph.D. dissertation. University of Göttingen, Göttingen, Germany.
König, C., Sammler, I., Wilde, E., Schlegel, H.G., 1969. Konstitutive Glucose-6-phosphat-dehydrogenase bei glucose verwertenden Mutanten von einem kryptischen Wildstamm [constitutive glucose-6-phosphate dehydrogenase in mutants utilizing glucose, which are derived from cryptic wildtype strains]. Arch. Mikrobiol. 67, 51–57.
Kourmentza, C., Plácido, J., Venetsaneas, N., Burniol-Figols, A., Varrone, C., Gavala, H. N., Reis, M.A.M., 2017. Recent advances and challenges towards sustainable polyhydroxyalkanoate (PHA) production. Bioengineering 4, 55. https://doi.org/10.3390/bioengineering4020055.
Kusian, B., Sültemeyer, D., Bowien, B., 2002. Carbonic anhydrase is essential for growth of *Ralstonia eutropha* at ambient CO_2 concentrations. J. Bacteriol. 184, 5018–5026. https://doi.org/10.1128/JB.184.18.5018-5026.2002.
Lambauer, V., Kratzer, R., 2022. Lab-scale cultivation of *Cupriavidus necator* on explosive gas mixtures: carbon dioxide fixation into polyhydroxybutyrate. Bioengineering 9, 204. https://doi.org/10.3390/bioengineering9050204.
Lambauer, V., Permann, A., Petrášek, Z., Subotić, V., Hochenauer, C., Kratzer, R., Reichhartinger, M., 2023. Automatic control of chemolithotrophic cultivation of *Cupriavidus necator*: optimization of oxygen supply for enhanced bioplastic production. Fermentation 9, 619. https://doi.org/10.3390/fermentation9070619.
Laycock, B., Halley, P., Pratt, S., Werker, A., Lant, P., 2014. The chemomechanical properties of microbial polyhydroxyalkanoates. Prog. Polym. Sci. 39, 397–442. https://doi.org/10.1016/j.progpolymsci.2013.06.008.
Lemoigne, M., 1926. Produit de deshydratation et de polymerisation de l'acide β-oxybutyrique. [Product of dehydration and polymerization of β-hydroxybutyric acid.]. Bull. Soc. Chim. Biol. 8, 770–782.
Lenz, O., Bernhard, M., Buhrke, T., Schwartz, E., Friedrich, B., 2002. The hydrogen-sensing apparatus in *Ralstonia eutropha*. J. Mol. Microbiol. Biotechnol. 4, 255–262.
Little, G.T., Ehsaan, M., Arenas-López, C., Jawed, K., Winzer, K., Kovacs, K., Minton, N. P., 2019. Complete genome sequence of *Cupriavidus necator* H16 (DSM 428). Microbiol. Resour. Announc. 8, e00814–e00819. https://doi.org/10.1128/MRA.00814-19.
Liu, Y.-P., Zheng, P., Sun, Z.-H., Ni, Y., Dong, J.-J., Zhu, L.-L., 2008. Economical succinic acid production from cane molasses by *Actinobacillus succinogenes*. Bioresour. Technol. 99, 1736–1742. https://doi.org/10.1016/j.biortech.2007.03.044.
Lopar, M., Vrana Špoljarić, I., Atlić, A., Koller, M., Braunegg, G., Horvat, P., 2013. Five-step continuous production of PHB analyzed by elementary flux, modes, yield space analysis and high structured metabolic model. Biochem. Eng. J. 79, 57–70. https://doi.org/10.1016/j.bej.2013.07.003.
Lopar, M., Špoljarić, I.V., Cepanec, N., Koller, M., Braunegg, G., Horvat, P., 2014. Study of metabolic network of *Cupriavidus necator* DSM 545 growing on glycerol by applying elementary flux modes and yield space analysis. J. Ind. Microbiol. Biotechnol. 41, 913–930. https://doi.org/10.1007/s10295-014-1439-y.
Makkar, N.S., Casida, L.E.Y., 1987. 1987. *Cupriavidus necator* gen. nov., sp. nov.; a nonobligate bacterial predator of bacteria in soil. Int. J. Syst. Evol. Microbiol. 37, 323–326. https://doi.org/10.1099/00207713-37-4-323.
Meng, D.-C., Shen, R., Yao, H., Chen, J.-C., Wu, Q., Chen, G.-Q., 2014. Engineering the diversity of polyesters. Curr. Opin. Biotechnol. 29, 24–33. https://doi.org/10.1016/j.copbio.2014.02.013.
Miu, D.-M., Eremia, M.C., Moscovici, M., 2022. Polyhydroxyalkanoates (PHAs) as biomaterials in tissue engineering: production, isolation, characterization. Mater. Basel Switz. 15, 1410. https://doi.org/10.3390/ma15041410.
Miura, Y., Okazaki, M., Ohi, K., Nishimura, T., 1981. Growth kinetics of hydrogen bacterium *Alcaligenes hydrogenophilus*. Agric. Biol. Chem. 45, 1181–1186. https://doi.org/10.1080/00021369.1981.10864681.
Miyahara, Y., Wang, C.-T., Ishii-Hyakutake, M., Tsuge, T., 2022. Continuous supply of non-combustible gas mixture for safe autotrophic culture to produce polyhydroxyalkanoate by hydrogen-oxidizing bacteria. Bioengineering 9, 586. https://doi.org/10.3390/bioengineering9100586.
Mori, J.F., Nagai, M., Kanaly, R.A., 2021. Complete genome sequence of *Cupriavidus necator* KK10, an azaarene-degrading and polyhydroxyalkanoate-producing soil bacterium. Microbiol. Resour. Announc. 10, e0042321 https://doi.org/10.1128/MRA.00423-21.
Moriuchi, R., Dohra, H., Kanesaki, Y., Ogawa, N., 2019. Complete genome sequence of 3-chlorobenzoate-degrading bacterium *Cupriavidus necator* NH9 and reclassification of the strains of the genera Cupriavidus and Ralstonia based on phylogenetic and whole-genome sequence analyses. Front. Microbiol. 10.
Mozumder, Md.S.I., Garcia-Gonzalez, L., Wever, H.D., Volcke, E.I.P., 2015. Poly(3-hydroxybutyrate) (PHB) production from CO_2: model development and process optimization. Biochem. Eng. J. 98, 107–116. https://doi.org/10.1016/j.bej.2015.02.031.
Nangle, S.N., Ziesack, M., Buckley, S., Trivedi, D., Loh, D.M., Nocera, D.G., Silver, P.A., 2020. Valorization of CO_2 through lithoautotrophic production of sustainable chemicals in *Cupriavidus necator*. Metab. Eng. 62, 207–220. https://doi.org/10.1016/j.ymben.2020.09.002.
Nonato, R., Mantelatto, P., Rossell, C., 2001. Integrated production of biodegradable plastic, sugar and ethanol. Appl. Microbiol. Biotechnol. 57, 1–5. https://doi.org/10.1007/s002530100732.
Obruca, S., Sedlacek, P., Slaninova, E., Fritz, I., Daffert, C., Meixner, K., Sedrlova, Z., Koller, M., 2020. Novel unexpected functions of PHA granules. Appl. Microbiol. Biotechnol. 104, 4795–4810. https://doi.org/10.1007/s00253-020-10568-1.
Orth, J.D., Thiele, I., Palsson, B.Ø., 2010. What is flux balance analysis? Nat. Biotechnol. 28, 245–248. https://doi.org/10.1038/nbt.1614.
Park, J.M., Kim, T.Y., Lee, S.Y., 2011. Genome-scale reconstruction and in silico analysis of the *Ralstonia eutropha* H16 for polyhydroxyalkanoate synthesis, lithoautotrophic growth, and 2-methyl citric acid production. BMC Syst. Biol. 5, 101. https://doi.org/10.1186/1752-0509-5-101.
Pearcy, N., Garavaglia, M., Millat, T., Gilbert, J.P., Song, Y., Hartman, H., Woods, C., Tomi-Andrino, C., Bommareddy, R.R., Cho, B.-K., Fell, D.A., Poolman, M., King, J.R., Winzer, K., Twycross, J., Minton, N.P., 2022. A genome-scale metabolic model of *Cupriavidus necator* H16 integrated with TraDIS and transcriptomic data reveals metabolic insights for biotechnological applications. PLoS Comput. Biol. 18, e1010106 https://doi.org/10.1371/journal.pcbi.1010106.
Peoples, O.P., Sinskey, A.J., 1989a. Fine structural analysis of the *Zoogloea ramigera* phbA-phbB locus encoding β-ketothiolase and acetoacetyl-CoA reductase: nucleotide

sequence of phbB. Mol. Microbiol. 3, 349–357. https://doi.org/10.1111/j.1365-2958.1989.tb00180.x.
Peoples, O.P., Sinskey, A.J., 1989b. Poly-β-hydroxybutyrate (PHB) biosynthesis in *Alcaligenes eutrophus* H16: identification and characterization of the PHB polymerase gene (phbC). J. Biol. Chem. 264, 15298–15303. https://doi.org/10.1016/S0021-9258(19)84825-1.
Peyraud, R., Cottret, L., Marmiesse, L., Gouzy, J., Genin, S., 2016. A resource allocation trade-off between virulence and proliferation drives metabolic versatility in the plant pathogen *Ralstonia solanacearum*. PLoS Pathog. 12, e1005939 https://doi.org/10.1371/journal.ppat.1005939.
Pfitzner, J., Schlegel, H.G., 1973. Denitrifikation bei *Hydrogenomonas eutropha* Stamm H16. [Denitrification in *Hydrogenomonas eutropha* strain H16.]. Arch. Für Mikrobiol. 90, 199–211. https://doi.org/10.1007/BF00424972.
Pham, N., van Heck, R.G.A., van Dam, J.C.J., Schaap, P.J., Saccenti, E., Suarez-Diez, M., 2019. Consistency, inconsistency, and ambiguity of metabolite names in biochemical databases used for genome-scale metabolic modelling. Metabolites 9, 28. https://doi.org/10.3390/metabo9020028.
Poehlein, A., Kusian, B., Friedrich, B., Daniel, R., Bowien, B., 2011. Complete genome sequence of the type strain *Cupriavidus necator* N-1. J. Bacteriol. 193, 5017. https://doi.org/10.1128/JB.05660-11.
Pohlmann, A., Fricke, W.F., Reinecke, F., Kusian, B., Liesegang, H., Cramm, R., Eitinger, T., Ewering, C., Pötter, M., Schwartz, E., Strittmatter, A., Voss, I., Gottschalk, G., Steinbüchel, A., Friedrich, B., Bowien, B., 2006. Genome sequence of the bioplastic-producing "Knallgas" bacterium *Ralstonia eutropha* H16. Nat. Biotechnol. 24, 1257–1262. https://doi.org/10.1038/nbt1244.
Povolo, S., Toffano, P., Basaglia, M., Casella, S., 2010. Polyhydroxyalkanoates production by engineered *Cupriavidus necator* from waste material containing lactose. Bioresour. Technol. 101, 7902–7907. https://doi.org/10.1016/j.biortech.2010.05.029.
Purama, R.K., Al-Sabahi, J.N., Sudesh, K., 2018. Evaluation of date seed oil and date molasses as novel carbon sources for the production of poly(3Hydroxybutyrate-co-3Hydroxyhexanoate) by *Cupriavidus necator* H16 Re 2058/pCB113. Ind. Crop. Prod. 119, 83–92. https://doi.org/10.1016/j.indcrop.2018.04.013.
Raberg, M., Peplinski, K., Heiss, S., Ehrenreich, A., Voigt, B., Döring, C., Bömeke, M., Hecker, M., Steinbüchel, A., 2011. Proteomic and transcriptomic elucidation of the mutant *Ralstonia eutropha* G+1 with regard to glucose utilization. Appl. Environ. Microbiol. 77, 2058–2070. https://doi.org/10.1128/AEM.02015-10.
Raberg, M., Voigt, B., Hecker, M., Steinbüchel, A., 2014. A closer look on the polyhydroxybutyrate- (PHB-) negative phenotype of *Ralstonia eutropha* PHB-4. PLoS One 9, e95907. https://doi.org/10.1371/journal.pone.0095907.
Reddy, C.S.K., Ghai, R., Rashmi, Kalia, V.C., 2003. Polyhydroxyalkanoates: an overview. Bioresour. Technol. 87, 137–146. https://doi.org/10.1016/S0960-8524(02)00212-2.
Repaske, R., 1962. The electron transport system of *Hydrogenomonas eutropha*: I. Diphosphopyridine nucleotide reduction by hydrogen. J. Biol. Chem. 237, 1351–1355. https://doi.org/10.1016/S0021-9258(18)60333-3.
Rivera-Briso, A.L., Serrano-Aroca, Á., 2018. Poly(3-hydroxybutyrate-co-3-hydroxyvalerate): enhancement strategies for advanced applications. Polymers 10. https://doi.org/10.3390/polym10070732.
Rochaix, J.-D., 2011. Regulation of photosynthetic electron transport. Biochim. Biophys. Acta BBA - Bioenerg. 1807, 375–383. https://doi.org/10.1016/j.bbabio.2010.11.010.
Rodríguez-Esperón, M.C., Eastman, G., Sandes, L., Garabato, F., Eastman, I., Iriarte, A., Fabiano, E., Sotelo-Silveira, J.R., Platero, R., 2022. Genomics and transcriptomics insights into luteolin effects on the beta-rhizobial strain *Cupriavidus necator* UYPR2.512. Environ. Microbiol. 24, 240–264. https://doi.org/10.1111/1462-2920.15845.
Saraiva, J.P., Bartholomäus, A., Kallies, R., Gomes, M., Bicalho, M., Kasmanas, J.C., Vogt, C., Chatzinotas, A., Stadler, P., Dias, O., da Rocha, U.N., 2021. OrtSuite: from genomes to prediction of microbial interactions within targeted ecosystem processes. Life Sci. Alliance 4. https://doi.org/10.26508/lsa.202101167.
Sauer, U., Canonaco, F., Heri, S., Perrenoud, A., Fischer, E., 2004. The soluble and membrane-bound transhydrogenases UdhA and PntAB have divergent functions in NADPH metabolism of *Escherichia coli*. J. Biol. Chem. 279, 6613–6619. https://doi.org/10.1074/jbc.M311657200.
Schlegel, H.G., Gottschalk, G., 1965. Utilization of glucose by a mutant of *Hydrogenomonas* H16. Biochem. Z. 341, 249–259.
Schlegel, H.G., Gottschalk, G., Von Bartha, R., 1961. Formation and utilization of poly-β-hydroxybutyric acid by Knallgas bacteria (*Hydrogenomonas*). Nature 191, 463–465. https://doi.org/10.1038/191463a0.
Schlegel, H.G., Lafferty, R., Krauss, I., 1970. The isolation of mutants not accumulating poly-beta-hydroxybutyric acid. Arch. Mikrobiol. 71, 283–294. https://doi.org/10.1007/BF00410161.
Schubert, P., Steinbüchel, A., Schlegel, H.G., 1988. Cloning of the *Alcaligenes eutrophus* genes for synthesis of poly-beta-hydroxybutyric acid (PHB) and synthesis of PHB in Escherichia coli. J. Bacteriol. 170, 5837–5847. https://doi.org/10.1128/jb.170.12.5837-5847.1988.
Schuster, S., Fell, D.A., Dandekar, T., 2000. A general definition of metabolic pathways useful for systematic organization and analysis of complex metabolic networks. Nat. Biotechnol. 18, 326–332. https://doi.org/10.1038/73786.
Schwab, H., Saurugger, P.N., Lafferty, R.M., 1983. Occurrence of deletion plasmids at high rates after conjugative transfer of the plasmids RP4 and RK2 from *Escherichia coli* to *Alcaligenes eutrophus* H16. Arch. Microbiol. 136, 140–146. https://doi.org/10.1007/BF00404789.
Schwartz, E., Henne, A., Cramm, R., Eitinger, T., Friedrich, B., Gottschalk, G., 2003. Complete nucleotide sequence of pHG1: a *Ralstonia eutropha* H16 megaplasmid encoding key enzymes of H_2-based ithoautotrophy and anaerobiosis. J. Mol. Biol. 332, 369–383. https://doi.org/10.1016/s0022-2836(03)00894-5.
Sen, K.Y., Hussin, M.H., Baidurah, S., 2019. Biosynthesis of poly(3-hydroxybutyrate) (PHB) by *Cupriavidus necator* from various pretreated molasses as carbon source. Biocatal. Agric. Biotechnol. 17, 51–59. https://doi.org/10.1016/j.bcab.2018.11.006.
Shimizu, R., Dempo, Y., Nakayama, Y., Nakamura, S., Bamba, T., Fukusaki, E., Fukui, T., 2015. New insight into the role of the calvin cycle: reutilization of CO_2 emitted through sugar degradation. Sci. Rep. 5, 11617. https://doi.org/10.1038/srep11617.
Shin, S.K., Ko, Y.J., Jeong, D.W., Lee, M.-E., You, S.K., Hyeon, J.E., Han, S.O., 2021. Enhanced production of polyhydroxybutyrate from syngas by using nanoscaled cellulose particles with a syngas-converting enzyme complex immobilized on *Ralstonia eutropha*. J. Clean. Prod. 285, 124903. https://doi.org/10.1016/j.jclepro.2020.124903.
Sichtig, H., Minogue, T., Yan, Y., Stefan, C., Hall, A., Tallon, L., Sadzewicz, L., Nadendla, S., Klimke, W., Hatcher, E., Shumway, M., Aldea, D.L., Allen, J., Koehler, J., Slezak, T., Lovell, S., Schoepp, R., Scherf, U., 2019. FDA-ARGOS is a database with public quality-controlled reference genomes for diagnostic use and regulatory science. Nat. Commun. 10, 3313. https://doi.org/10.1038/s41467-019-11306-6.
Siddiqui, R.A., Warnecke-Eberz, U., Hengsberger, A., Schneider, B., Kostka, S., Friedrich, B., 1993. Structure and function of a periplasmic nitrate reductase in *Alcaligenes eutrophus* H16. J. Bacteriol. 175, 5867–5876. https://doi.org/10.1128/jb.175.18.5867-5876.1993.
Sohn, Y.J., Son, J., Jo, S.Y., Park, S.Y., Yoo, J.I., Baritugo, K.-A., Na, J.G., Choi, J., Kim, H.T., Joo, J.C., Park, S.J., 2021. Chemoautotroph *Cupriavidus necator* as a potential game-changer for global warming and plastic waste problem: a review. Bioresour. Technol. 340, 125693. https://doi.org/10.1016/j.biortech.2021.125693.
Song, H.-S., Ramkrishna, D., 2009. Reduction of a set of elementary modes using yield analysis. Biotechnol. Bioeng. 102, 554–568. https://doi.org/10.1002/bit.22062.
Song, H.-S., Morgan, J.A., Ramkrishna, D., 2009. Systematic development of hybrid cybernetic models: application to recombinant yeast co-consuming glucose and xylose. Biotechnol. Bioeng. 103, 984–1002. https://doi.org/10.1002/bit.22332.
Spaans, S., Weusthuis, R., Van Der Oost, J., Kengen, S., 2015. NADPH-generating systems in bacteria and archaea. Front. Microbiol. 6.
Špoljarić, I.V., Lopar, M., Koller, M., Muhr, A., Salerno, A., Reiterer, A., Horvat, P., 2013. In silico optimization and low structured kinetic model of poly[(R)-3-hydroxybutyrate] synthesis by *Cupriavidus necator* DSM 545 by fed-batch cultivation on glycerol. J. Biotechnol. 168, 625–635. https://doi.org/10.1016/j.jbiotec.2013.08.019.
Steinbüchel, A., Hustede, E., Liebergesell, M., Pieper, U., Timm, A., Valentin, H., 1992. Molecular basis for biosynthesis and accumulation of polyhydroxyalkanoic acids in bacteria. FEMS Microbiol. Rev. 9, 217–230. https://doi.org/10.1111/j.1574-6968.1992.tb05841.x.
Strittmatter, C.S., Eggers, J., Biesgen, V., Pauels, I., Becker, F., Steinbüchel, A., 2022. The reliance of glycerol utilization by *Cupriavidus necator* on CO_2 fixation and improved glycerol catabolism. Appl. Microbiol. Biotechnol. 106, 2541–2555. https://doi.org/10.1007/s00253-022-11842-0.
Strøm-Andersen, S.B., Brekke, Andreas, Strange, Louise, Nhat, 2019. Valorisation of whey: A tale of two Nordic dairies. In: From Waste to Value. Routledge.
Sudesh, K., Abe, H., Doi, Y., 2000. Synthesis, structure and properties of polyhydroxyalkanoates: biological polyesters. Prog. Polym. Sci. 25, 1503–1555. https://doi.org/10.1016/S0079-6700(00)00035-6.
Sun, C., Pérez-Rivero, C., Webb, C., Theodoropoulos, C., 2020. Dynamic metabolic analysis of *Cupriavidus necator* DSM545 producing poly(3-hydroxybutyric acid) from glycerol. Processes 8, 657. https://doi.org/10.3390/pr8060657.
Taga, N., Tanaka, K., Ishizaki, A., 1997. Effects of rheological change by addition of carboxymethylcellulose in culture media of an air-lift fermentor on poly-D-3-hydroxybutyric acid productivity in autotrophic culture of hydrogen-oxidizing bacterium, *Alcaligenes eutrophus*. Biotechnol. Bioeng. 53, 529–533. https://doi.org/10.1002/(SICI)1097-0290(19970305)53:5<529::AID-BIT11>3.0.CO;2-B.
Tanaka, K., Ishizaki, A., Kanamaru, T., Kawano, T., 1995. Production of poly(D-3-hydroxybutyrate) from CO_2, H_2, and O_2 by high cell density autotrophic cultivation of *Alcaligenes eutrophus*. Biotechnol. Bioeng. 45, 268–275. https://doi.org/10.1002/bit.260450312.
Tanaka, K., Yoshida, K., Orita, I., Fukui, T., 2021. Biosynthesis of poly(3-hydroxybutyrate-co-3-hydroxyhexanoate) from CO_2 by a recombinant *Cupriavidus necator*. Bioengineering 8, 179. https://doi.org/10.3390/bioengineering8110179.
Tang, R., Weng, C., Peng, X., Han, Y., 2020. Metabolic engineering of *Cupriavidus necator* H16 for improved chemoautotrophic growth and PHB production under oxygen-limiting conditions. Metab. Eng. 61, 11–23. https://doi.org/10.1016/j.ymben.2020.04.009.
Ternon, C., Grousseau, E., Gunther, J., Gorret, N., Guillouet, S., Sinskey, A.J., Aceves-Lara, C.A., Roux, G., 2014. Dynamic model for isopropanol production by *Cupriavidus necator*. In: IFAC Proc. Vol., 19th IFAC World Congress, 47, pp. 4388–4393. https://doi.org/10.3182/20140824-6-ZA-1003.02267.
Unrean, P., Tee, K.L., Wong, T.S., 2019. Metabolic pathway analysis for in silico design of efficient autotrophic production of advanced biofuels. Bioresour. Bioprocess. 6, 49. https://doi.org/10.1186/s40643-019-0282-4.
Utsunomia, C., Ren, Q., Zinn, M., 2020. Poly(4-hydroxybutyrate): current state and perspectives. Front. Bioeng. Biotechnol. 8.
Van der Linden, E., Burgdorf, T., Bernhard, M., Bleijlevens, B., Friedrich, B., Albracht, S.P.J., 2004. The soluble [NiFe]-hydrogenase from *Ralstonia eutropha* contains four cyanides in its active site, one of which is responsible for the insensitivity towards oxygen. JBIC J. Biol. Inorg. Chem. 9, 616–626. https://doi.org/10.1007/s00775-004-0555-y.

Vandamme, P., Coenye, T., 2004. Taxonomy of the genus *Cupriavidus*: a tale of lost and found. Int. J. Syst. Evol. Microbiol. 54, 2285–2289. https://doi.org/10.1099/ijs.0.63247-0.

Vaneechoutte, M., Kämpfer, P., De Baere, T., Falsen, E., Verschraegen, G., 2004. *Wautersia* gen. nov., a novel genus accommodating the phylogenetic lineage including *Ralstonia eutropha* and related species, and proposal of *Ralstonia* [*Pseudomonas*] *syzygii* (Roberts et al. 1990) comb. nov. Int. J. Syst. Evol. Microbiol. 54, 317–327. https://doi.org/10.1099/ijs.0.02754-0.

Virtanen, P., Gommers, R., Oliphant, T.E., Haberland, M., Reddy, T., Cournapeau, D., Burovski, E., Peterson, P., Weckesser, W., Bright, J., van der Walt, S.J., Brett, M., Wilson, J., Millman, K.J., Mayorov, N., Nelson, A.R.J., Jones, E., Kern, R., Larson, E., Carey, C.J., Polat, İ., Feng, Y., Moore, E.W., VanderPlas, J., Laxalde, D., Perktold, J., Cimrman, R., Henriksen, I., Quintero, E.A., Harris, C.R., Archibald, A.M., Ribeiro, A. H., Pedregosa, F., van Mulbregt, P., 2020. SciPy 1.0: fundamental algorithms for scientific computing in Python. Nat. Methods 17, 261–272. https://doi.org/10.1038/s41592-019-0686-2.

Volova, T., Kalacheva, G., Altukhova, O., 2002. Autotrophic synthesis of polyhydroxyalkanoates by the bacteria *Ralstonia eutropha* in the presence of carbon monoxide. Appl. Microbiol. Biotechnol. 58, 675–678. https://doi.org/10.1007/s00253-002-0941-8.

Weightman, A.J., Don, R.H., Lehrbach, P.R., Timmis, K.N., 1984. The identification and cloning of genes encoding haloaromatic catabolic enzymes and the construction of hybrid pathways for substrate mineralization. In: Omenn, G.S., Hollaender, A., Chakrabarty, A.M., Levin, M., Nester, E., Orians, G.H., Wilson, C.M. (Eds.), Genetic Control of Environmental Pollutants, Basic Life Sciences. Springer US, Boston, MA, pp. 47–80. https://doi.org/10.1007/978-1-4684-4715-6_4.

Wheeler, T.J., Eddy, S.R., 2013. Nhmmer: DNA homology search with profile HMMs. Bioinformatics 29, 2487–2489. https://doi.org/10.1093/bioinformatics/btt403.

Wittich, R.-M., Wolff, P., 2007. Growth of the genetically engineered strain *Cupriavidus necator* RW112 with chlorobenzoates and technical chlorobiphenyls. Microbiol. Read. Engl. 153, 186–195. https://doi.org/10.1099/mic.0.29096-0.

Xie, Z., Wang, D., Ben Fekih, I., Yu, Y., Li, Y., Alwathnani, H., Herzberg, M., Rensing, C., 2023. Whole genome sequence analysis of *Cupriavidus necator* C39, a multiple heavy metal(loid) and antibiotic resistant bacterium isolated from a gold/copper mine. Microorganisms 11, 1518. https://doi.org/10.3390/microorganisms11061518.

Yabuuchi, E., Kosako, Y., Yano, I., Hotta, H., Nishiuchi, Y., 1995. Transfer of two *Burkholderia* and an *Alcaligenes* species to *Ralstonia* gen. Nov. Microbiol. Immunol. 39, 897–904. https://doi.org/10.1111/j.1348-0421.1995.tb03275.x.

Yonezuka, K., Shimodaira, J., Tabata, M., Nagase, S., Kasai, D., Hosoyama, A., Yamazoe, A., Fujita, N., Fukuda, M., 2016. Draft genome sequence of a chlorinated-ethene degrader, *Cupriavidus necator* strain PHE3-6 (NBRC 110655). Genome Announc. 4 https://doi.org/10.1128/genomeA.01743-15 e01743–15.

Yousuf, R.G., Winterburn, J.B., 2016. Date seed characterisation, substrate extraction and process modelling for the production of polyhydroxybutyrate by *Cupriavidus necator*. Bioresour. Technol. 222, 242–251. https://doi.org/10.1016/j.biortech.2016.09.107.

Yu, J., Dow, A., Pingali, S., 2013. The energy efficiency of carbon dioxide fixation by a hydrogen-oxidizing bacterium. Int. J. Hydrog. Energy 38, 8683–8690. https://doi.org/10.1016/j.ijhydene.2013.04.153.

Zarnt, G., Schräder, T., Andreesen, J.R., 1997. Degradation of tetrahydrofurfuryl alcohol by *Ralstonia eutropha* is initiated by an inducible pyrroloquinoline quinone-dependent alcohol dehydrogenase. Appl. Environ. Microbiol. 63, 4891–4898. https://doi.org/10.1128/aem.63.12.4891-4898.1997.

Zhang, J., Shishatskaya, E.I., Volova, T.G., da Silva, L.F., Chen, G.-Q., 2018. Polyhydroxyalkanoates (PHA) for therapeutic applications. Mater. Sci. Eng. C 86, 144–150. https://doi.org/10.1016/j.msec.2017.12.035.

Zhila, N.O., Sapozhnikova, K.Y., Kiselev, E.G., Vasiliev, A.D., Nemtsev, I.V., Shishatskaya, E.I., Volova, T.G., 2021. Properties of degradable polyhydroxyalkanoates (PHAs) synthesized by a new strain, *Cupriavidus necator* IBP/SFU-1, from various carbon sources. Polymers 13, 3142. https://doi.org/10.3390/polym13183142.

Zuñiga, C., Li, C.-T., Huelsman, T., Levering, J., Zielinski, D.C., McConnell, B.O., Long, C. P., Knoshaug, E.P., Guarnieri, M.T., Antoniewicz, M.R., Betenbaugh, M.J., Zengler, K., 2016. Genome-scale metabolic model for the green alga *Chlorella vulgaris* UTEX 395 accurately predicts phenotypes under autotrophic, heterotrophic, and mixotrophic growth conditions. Plant Physiol. 172, 589–602. https://doi.org/10.1104/pp.16.00593.